R. & M. No. 3047
~~(18,946)~~ 18486
A.R.C. Technical Report

MINISTRY OF SUPPLY

AERONAUTICAL RESEARCH COUNCIL
REPORTS AND MEMORANDA

A Numerical Method for Calculating the Starting and Perturbation of a Two-dimensional Jet at Low Reynolds Number

By

R. B. PAYNE
Department of Mathematics, University of Manchester

LONDON: HER MAJESTY'S STATIONERY OFFICE
1958
PRICE 17s. 6d. NET

A Numerical Method for Calculating the Starting and Perturbation of a Two-dimensional Jet at Low Reynolds Number

By

R. B. PAYNE

Department of Mathematics, University of Manchester

Reports and Memoranda No. 3047

June, 1956

1. *Introduction.*—1.1. *Aim.*—The number of available exact solutions of the full equations of motion of an incompressible viscous fluid is remarkably few. Those that exist are mostly limited to steady flows. Where a steady state solution does exist, one may be able to obtain a little information about the corresponding unsteady flow by the method of small perturbations. However, in the interesting case of instability, this only shows how a small disturbance behaves initially. The subsequent stages of chaotic motion, as the laminar flow 'breaks up', have attracted the attention of many but still largely remain a source of fascination rather than a field for fruitful research. Only when the flow becomes completely turbulent can the theories of turbulence be applied. These theories do not discuss the origin of turbulence, still leaving the gap in the present state of knowledge between small perturbation theory and turbulence.

There is, therefore, a great need for a method of attacking directly the full equations of motion of an unsteady viscous flow. Recent advances in high speed electronic computers make available a powerful device for performing the computations. The lack of some such calculating robot has no doubt discouraged earlier attempts to adopt this approach.

Since with any electronic computer one has available only a finite storage space, the possibility of solving a completely three-dimensional problem is perhaps a little ambitious at present. Further, from turbulence theory it is known that large eddies have a tendency to break into smaller eddies limited only by viscosity. Hence, in order to follow numerically a turbulent flow, a large number of closely spaced mesh points would be required to include both the large scale and small scale effects. It is therefore necessary to confine the range of eddy sizes, so that a suitably low Reynolds number must be chosen.

Of two-dimensional problems, the two most suitable viscous flows appeared to be:

(*a*) the flow past a cylinder

(*b*) the plane jet.

The latter was chosen because of the simplicity of the image vortex system required to satisfy the boundary condition. The method could also be applied to the flow past a circular cylinder and the formation of the Kármán vortex street.

The following is a finite-difference method of solving the equations of motion of an unsteady, viscous (and consequently rotational) flow, with particular reference to the starting and perturbation of a plane jet, for which results were obtained.

1.2. *Numerical Methods.*—It was proposed to use Helmholtz's vorticity equation:

$$\frac{\partial \omega}{\partial t} + u\frac{\partial \omega}{\partial x} + v\frac{\partial \omega}{\partial y} = \nu\left(\frac{\partial^2 \omega}{\partial x^2} + \frac{\partial^2 \omega}{\partial y^2}\right),$$

where ω = vorticity, to determine the vorticity at successive small intervals of time. The earliest attempt to solve parabolic partial differential equations is due to L. F. Richardson in 1910. Although later writers have adversely criticised this treatise, Richardson's work is the basis of many subsequent investigations. A notable modern development is that due to P. D. Lax who overcomes the instability difficulties (*see* section 4.2) by introducing an ' artificial viscosity '. It was impossible to use the Lax method here since the artificial viscosity would be about 20 times as large as the viscosity it was desired to use. However, in Lax's paper is shown the desirability of using equations in ' conservation form ', so that the vorticity equation in the form:

$$\frac{\partial \omega}{\partial t} + \frac{\partial (u\omega)}{\partial x} + \frac{\partial (v\omega)}{\partial y} = \nu\left(\frac{\partial^2 \omega}{\partial x^2} + \frac{\partial^2 \omega}{\partial y^2}\right)$$

was used here to advantage.

Similar equations occur in meteorological problems (but it is not usual to include viscosity). The solution is obtained after making suitable simplifying approximations which are valid for the atmosphere.

1.3. *The Plane Jet.*—The presence of vorticity makes it desirable to be able to use Helmholtz's equations for the velocity due to a point vortex to determine the velocity (Lamb, p. 219). By considering a flow in a half-plane, the condition that no fluid crosses a solid boundary is easily satisfied by the method of images.

Now for a plane jet the boundary is as shown in Fig. 1. To obtain the velocity due to a point vortex at P by introducing an image vortex at P', is equivalent to replacing the boundary by the half-plane YY' (without the orifice). This approximation is valid if the effect of the vortex at P does not reach far into the entry channel. Now the stream function, ψ, for an irrotational flow satisfies:

$$\frac{\partial^2 \psi}{\partial x^2} + \frac{\partial^2 \psi}{\partial y^2} = 0.$$

Therefore, in the entry channel:

$$\psi = \sum_{n=0}^{\infty} A_n \cos{(2n+1)\pi y/d} \exp{\{(2n+1)\pi x/d\}}$$

$$+ \sum_{n=1}^{\infty} B_n \sin{2n\pi y/d} \exp{\{2n\pi x/d\}}$$

(ψ = constant when $y = \pm d/2$ and $\psi \to 0$ as $x \to -\infty$).

The predominating term in ψ is $A_0 \cos{(\pi y/d)} \exp{(\pi x/d)}$, which at $-x = d/2$ is $\exp{(-\pi/2)} = 1/4{\cdot}8$ of its value at $x = 0$; at $-x = d$ is $1/23$ of its value at $x = 0$; at $-x = 2d$ is $1/535$ of its value at $x = 0$.

Further, the condition that in a viscous flow there is zero velocity at a solid boundary (relative to the boundary) is satisfied by the generation of additional vorticity at the boundary.

In his investigation of edge-tones, Curle found the vorticity generated at the orifice was important. His argument was that if the jet is deflected (Fig. 2), the flow turns through a greater angle at A than at B. Hence the velocity near A is greater than the velocity near B, which gives greater shear and therefore more vorticity at A. To obtain a quantitative estimate of this vorticity the boundary condition that the velocity component, v, = 0 at the orifice was taken, it

being assumed that the fluid in the entry channel continues in undisturbed uniform flow. Just as at the solid wall, this condition was satisfied by the generation of additional vorticity (Fig. 3). This gives vorticity of the same sign as does Curle's argument.

A steady state solution for a plane laminar jet has been obtained by Bickley by finding an exact similarity solution of the boundary-layer equations. Savic has applied small perturbations to Bickley's solution.

1.4. *Method.*—The half-plane is covered by a lattice of mesh points. The space derivatives in the vorticity equation (1) are approximated by the difference in the vorticity at the appropriate neighbouring points of the mesh divided by the distance between them. The time derivative is also approximated by the difference in vorticity at two different times divided by the small increment of time. Hence we have an equation which gives explicitly the vorticity at successive small intervals of time.

At each time step it is necessary to find the velocity at the lattice points. There are two factors which determine the velocity: the rate of inflow of fluid at the boundary and the distribution of vorticity, the two effects being additive. The effect of the flow at the orifice may be expressed as an integral along the boundary, YOY', of a simple source flow (Lamb, chapters 3 and 7). This integral is calculated by taking the sum of the effects of small elements of the boundary. The effect of the vorticity is calculated by replacing the continuous distribution of vorticity by a series of point vortices at the mesh points and adding the effects of these point vortices. Helmholtz's equations are used to find the effect of each point vortex.

1.5. *First Attempts and Improvements.*—At the outset it was felt that starting the jet impulsively from rest would severely tax a numerical method. As a compromise, in the first runs the velocity at the orifice was increased linearly with time to its maximum value (Fig. 4).

It was found that after the velocity stopped increasing (at A) the vorticity continued to increase until it reached a maximum and then decreased, symmetrical oscillations being set up (*see* Graph 14). Increasing t_A merely reduced the size of the oscillations. Also using a smaller time interval did not eliminate these oscillations. A slight improvement was affected by smoothing off the corners at O and A (Fig. 10). The size of these oscillations increased with Reynolds number.

A more stable finite-difference scheme was sought and the one chosen (section 2.7) is similar to that used by Bushby and to a scheme which can be used for ordinary differential equations. It consists, essentially, of using a forward time difference to get a first approximation to the vorticity and then getting a second approximation using a central time difference. Stability of the finite-difference equation is discussed in section 4.2 where a critical time interval (depending on the Reynolds number) is obtained above which the difference equation is unstable (Graph 20).

Further improvements which were incorporated in the course of these preliminary tries were:

(*a*) The use of the ' conservation form ' of the vorticity equation (*cf.* Lax, and *see* section 4.6 on the conservation of vorticity)

(*b*) The use of a more accurate finite difference approximation for the space derivative in the direction perpendicular to the jet. In general, changes were more rapid in this direction than in the direction of the jet (section 2.7).

Also it was convenient to have eleven points across the jet (section 6.5). It was necessary to experiment with various values of the ratio of the diameter of the orifice to the width of the extreme mesh lines before the value 0·4 was chosen.

1.6. *The Curved Mesh.*—It was decided to use a curved mesh, consisting of ellipses and hyperbolae, rather than a rectangular mesh. This had the advantage that fewer mesh points were required at the expense of dealing with more complicated equations. The method will be described for a rectangular mesh and the curvilinear co-ordinates introduced in section 6. Near the orifice there is little difference between the rectangular and curved meshes.

1.7. *Results.*—The starting of a symmetrical jet is displayed in Graphs 1 to 5 which show the vorticity distribution and the streamlines at successive times. At first the fluid moves radially from the orifice but, as vorticity spreads into the half-plane, the flow soon takes the characteristic mushroom shape. As t increases the mushroom grows, the front whirls leaving behind them a steady flow. This steady flow is similar to Bickley's steady state solution (Graph 6). Andrade's correction to Bickley's solution does not improve the agreement.

At higher Reynolds numbers, numerical instability began to appear in the results as is seen from Graph 14 where the vorticity at particular points is plotted against time for Reynolds numbers 150 (*see* section 7.4).

Unsymmetry was produced by introducing a small perturbation at the orifice. Three frequencies of sinusoidal oscillations were used and it was found that the lowest frequency produced the greatest oscillation of the jet (*see* section 7.5). This lowest frequency ($f = 5$) was greater than the frequency of edge-tones (Wood's formula for the frequency of edge tones gives $f = 0{\cdot}055\ U/d = 0{\cdot}89$).

A more detailed description of results is given in section 7.

Tables of vorticity, etc., are not included in this paper but are obtainable in the author's Ph.D. Thesis at the University of Manchester.

2. *Complete Statement of the Problem.*—2.1. *Differential Equation of Motion.*—The flow of an incompressible viscous fluid in a half-plane is considered. The boundary of the half-plane is an infinite solid wall on either side of an orifice of width d.

Take rectangular axes, OX along the line of symmetry and OY along the boundary, and let $u(x,y,t)$, $v(x,y,t)$ be the components of velocity (Fig. 1). Let ω = the vorticity = $(\partial v/\partial x) - (\partial u/\partial y)$. We have (Lamb, p. 578):

$$\frac{\partial \omega}{\partial t} + u\frac{\partial \omega}{\partial x} + v\frac{\partial \omega}{\partial y} = \nu\left(\frac{\partial^2 \omega}{\partial x^2} + \frac{\partial^2 \omega}{\partial y^2}\right), \qquad (1)$$

where ν = the coefficient of viscosity. Since the fluid is incompressible:

$$\frac{\partial u}{\partial x} + \frac{\partial v}{\partial y} = 0\,. \qquad (2)$$

Adding equation (2) multiplied by ω to equation (1):

$$\frac{\partial \omega}{\partial t} + \frac{\partial}{\partial x}(u\omega) + \frac{\partial}{\partial y}(v\omega) = \nu\left(\frac{\partial^2 \omega}{\partial x^2} + \frac{\partial^2 \omega}{\partial y^2}\right). \qquad (3)$$

2.2. *Boundary Conditions.*—The boundary was taken as the plane YOY' consisting of:

(a) the solid wall, $x = 0$, $|y| \geqslant d/2$,

(b) the orifice, $x = 0$, $|y| \leqslant d/2$,

where d is the width of the orifice. The conditions to be satisfied at the boundary ($x = 0$) were:

$$u(0,y,t) = u_0(y,t) \qquad (4)$$

$$v(0,y,t) = 0 \qquad (5)$$

for all y and t, where $u_0(y,t)$ is prescribed for all t and is zero for all y such that $|\,y\,| \geqslant d/2$.

These boundary conditions imply that the effect of the flow in the half-plane, $x > 0$, on the flow in the entry channel has been neglected. In section 1.3 this effect was shown to be small.

As was shown in section 1.4 condition (4) implies that the velocity at any point may be found by adding:

(i) the effect of the vorticity distribution (including the image vorticity)

(ii) the effect of the source flow (*see* section 2.4).

Condition (5) implies the generation of additional vorticity at the boundary, both at the solid wall and at the orifice (*see* sections 1.3 and 2.5).

2.3. *Mesh Points.*—Consider a set of mesh points, $x = k\,\Delta x$, $y = j\,\Delta y$, $t = n\,\Delta t$, where k, j, and n are integers and where $\Delta x = \Delta y =$ constant, $\Delta t =$ constant. Replacing the derivatives in equation (3) by finite differences such as:

$$\frac{\partial \omega}{\partial t} = \frac{1}{\Delta t}\{\omega(x,y,t+\Delta t) - \omega(x,y,t)\},$$

$$\frac{\partial a}{\partial x} = \frac{1}{2\Delta x}\{a(x+\Delta x,y,t) - a(x-\Delta x,y,t)\} \text{ where } a = u\omega,$$

$$\frac{\partial b}{\partial y} = \frac{1}{2\Delta y}\{b(x,y+\Delta y,t) - b(x,y-\Delta y,t)\} \text{ where } b = v\omega, \qquad (6)$$

$$\frac{\partial^2 \omega}{\partial x^2} = \frac{1}{\Delta x^2}\{\omega(x+\Delta x,y,t) - 2\omega(x,y,t) + \omega(x-\Delta x,y,t)\},$$

$$\frac{\partial^2 \omega}{\partial y^2} = \frac{1}{\Delta y^2}\{\omega(x,y+\Delta y,t) - 2\omega(x,y,t) + \omega(x,y-\Delta y,t)\},$$

one obtains an equation of the form:

$$\omega(x,y,t+\Delta t) = \omega(x,y,t) + f\{u(X,Y,t),\, v(X,Y,t),\, \omega(X,Y,t)\}, \qquad (7)$$

in which X takes the values $x \pm \Delta x$, x, and Y takes the values $y \pm \Delta y$, y.

Or, using the notation:

$$\phi^{(n)}_{k,j} = \phi(k\,\Delta x,\, j\,\Delta y,\, n\,\Delta t),$$

equation (7) can be written:

$$\omega^{(n+1)}_{k,j} = \omega^{(n)}_{k,j} + f\{u^{(n)}_{K,J},\, v^{(n)}_{K,J},\, \omega^{(n)}_{K,J}\}, \qquad (7a)$$

in which K takes the values $k \pm 1$, k, and J takes the values $j \pm 1$, j, and where:

$$f = \frac{\Delta t}{2\Delta x}\left(u^{(n)}_{k-1,j}\,\omega^{(n)}_{k-1,j} - u^{(n)}_{k+1,j}\,\omega^{(n)}_{k+1,j} + v^{(n)}_{k,j-1}\,\omega^{(n)}_{k,j-1} - v^{(n)}_{k,j+1}\,\omega^{(n)}_{k,j+1}\right)$$

$$+ \nu\,\frac{\Delta t}{\Delta x^2}\left(\omega^{(n)}_{k+1,j} + \omega^{(n)}_{k-1,j} + \omega^{(n)}_{k,j+1} + \omega^{(n)}_{k,j-1} - 4\omega^{(n)}_{k,j}\right).$$

Hence, if ω and u, v are known at time, t, at all points of the space mesh $k \geqslant 0$ and $-\infty < j < \infty$, then equation (7) gives ω at time $t + \Delta t$ at all points such that $k \geqslant 1$ and $-\infty < j < \infty$.

2.4. *Determination of Velocity.*—In order to be able to proceed with the numerical integration by repeated use of the difference equation (7), it is necessary to be able to determine the velocity when the vorticity distribution is given. The velocity u, v due to the vorticity is given by:

$$u(x,y,t) = -\frac{1}{2\pi}\int\int_{-\infty}^{\infty} \omega(X,Y,t)\,\frac{(y-Y)}{(x-X)^2+(y-Y)^2}\,dX\,dY$$

$$v(x,y,t) = \frac{1}{2\pi}\int\int_{-\infty}^{\infty} \omega(X,Y,t)\,\frac{(x-X)}{(x-X)^2+(y-Y)^2}\,dX\,dY$$

(Lamb, p. 219) in which $\omega(X,Y,t)$ for X negative (the image vorticity) is defined as $-\omega(-X,Y,t)$. These integrals are evaluated by replacing the continuous distribution of vorticity in the square:

$$m\,\Delta x - \Delta x/2 < X < m\,\Delta x + \Delta x/2$$

$$l\,\Delta y - \Delta y/2 < Y < l\,\Delta y + \Delta y/2$$

by a point vortex at the point P $(m\,\Delta x, l\,\Delta y)$ of strength $\omega^{(n)}_{m,l}\,\Delta x\,\Delta y$ (Fig. 5).

Hence the velocity at the point $Q(k\,\Delta x, j\,\Delta y)$ due to the vorticity is given by:

$$\left.\begin{aligned} u^{(n)}_{k,j} &= \left(\sum_{m=-\infty}^{-1} + \sum_{m=1}^{\infty}\right)\sum_{l=-\infty}^{\infty} A_{k-m,j-l}\,\omega^{(n)}_{m,l}\,, \\ v^{(n)}_{k,j} &= \left(\sum_{m=-\infty}^{-1} + \sum_{m=1}^{\infty}\right)\sum_{l=-\infty}^{\infty} D_{k-m,j-l}\,\omega^{(n)}_{k,l}\,, \end{aligned}\right\} \quad \ldots \quad \ldots \quad \ldots \quad (8)$$

where $$A_{a,b} = -\frac{\Delta x}{2\pi}\cdot\frac{b}{a^2+b^2} \text{ if } a^2+b^2 \neq 0,$$

$$D_{a,b} = +\frac{\Delta x}{2\pi}\cdot\frac{a}{a^2+b^2} \text{ if } a^2+b^2 \neq 0,$$

and $$A_{0,0} = D_{0,0} = 0.$$

Because of the inclusion of the image vortices in equations (8) the first of the two equations gives $u = 0$ on the boundary $(k = 0)$.

The effect on the velocity at the point Q due to the inflow at the boundary is given by:

$$u(x,y,t) = \frac{2}{2\pi}\int_{Y=-\infty}^{\infty} u_0(Y,t)\,\frac{x}{x^2+(y-Y)^2}\,dY$$

$$v(x,y,t) = \frac{2}{2\pi}\int_{Y=-\infty}^{\infty} u_0(Y,t)\,\frac{(y-Y)}{x^2+(y-Y)^2}\,dY$$

(Lamb, p. 64). These integrals are similarly evaluated by replacing the inflow through the element of the boundary, $l\,\Delta y - \Delta y/2 \leqslant Y \leqslant l\,\Delta y + \Delta y/2$, by a point source of strength $2\bar{u}_0(l\,\Delta y, n\,\Delta t)$ (Fig. 6). Δy at the point $S(o, l\,\Delta y)$ where $\bar{u}_0(l\,\Delta y, n\,\Delta t)$ is the average value of

$u_0(Y, n\,\Delta t)$ for this element of the boundary. Hence the velocity at the point Q due to the source flow at the boundary is given by:

$$\left.\begin{aligned} u_{k,j}^{(n)} &= \sum_{l=-\infty}^{\infty} C_{k,j,l}\,\bar{u}_0(l\,\Delta y,\, n\,\Delta t) \\ v_{k,j}^{(n)} &= \sum_{l=-\infty}^{\infty} F_{k,j,l}\,\bar{u}_0(l\,\Delta y,\, n\,\Delta t) \end{aligned}\right\} \quad . \qquad .. \qquad .. \qquad .. \qquad .. \qquad (10)$$

where $$C_{k,j,l} = \frac{1}{\pi}\cdot\frac{k}{k^2+(j-l)^2} \text{ if } k^2+(j-l)^2 \neq 0$$

$$F_{k,j,l} = \frac{1}{\pi}\cdot\frac{(j-l)}{k^2+(j-l)^2} \text{ if } k^2+(j-l)^2 \neq 0$$

and $$C_{0,j,l} = 1 \text{ if } j = l$$

$$F_{0,j,l} = 0 \text{ if } j = l.$$

The complete velocity at the point Q is given by the sum of the vorticity terms (8) and the source flow terms (10). It is unnecessary to include in the source flow points where $\bar{u}_0(y,t) = 0$ (we have $u_0(y,t) = 0$ for $|y| \geqslant d/2$) so that the sums (10) are over a finite number of points only. Similarly in the vorticity terms (8), points where the vorticity is zero make zero contribution. Hence the complete velocity is:

$$\left.\begin{aligned} u_{k,j}^{(n)} &= \left(\sum_{m=-m_0}^{-1} + \sum_{m=1}^{m_0}\right)\sum_{l=-l_0}^{l_0} A_{k-m,j-l}\,\omega_{m,l}^{(n)} + \sum_{l=-l_1}^{l_1} C_{k,j,l}\,\bar{u}_0(l\,\Delta y,\, n\,\Delta t) \\ v_{k,j}^{(n)} &= \left(\sum_{m=-m_0}^{-1} + \sum_{m=1}^{m_0}\right)\sum_{l=-l_0}^{l_0} D_{k-m,j-l}\,\omega_{m,l}^{(n)} + \sum_{l=-l_1}^{l_1} F_{k,j,l}\,\bar{u}_0(l\,\Delta y,\, n\,\Delta t) \end{aligned}\right\} \quad .. \qquad .. \qquad (11)$$

where the effect of vorticity at points such that $m > m_0$ or $l > l_0$ has been neglected.

2.5. *Vorticity Generated at the Boundary.*—If the method of section 2.4 is used to evaluate the velocity at points Q on the boundary ($k = 0$), the vortices give zero contribution to u (since the image vortex has an equal and opposite effect) but a non-zero contribution to v. (The contribution from the image vortices is equal to the contribution from the vortices themselves, so it is sufficient only to find the effect of the vortices themselves and multiply the result by two). The point sources also give a zero contribution to u but a non-zero contribution to v, except when $S = Q$ in which case (9) is replaced by a contribution, $\bar{u}_0(l\,\Delta y,\, n\,\Delta t)$, to u and zero to v. Hence the boundary condition, $u(0,y,t) = u_0(y,t)$, is satisfied but the condition, $v(0,y,t) = 0$, would appear to be violated in general. The condition, $v(0,y,t) = 0$, is enforced by considering the velocity component, v, to generate additional vorticity at the boundary. Suppose $v_{0,j}^{(n)}$ is the velocity component obtained from equation (11) at the point P $(0, j\,\Delta y)$.

Let A be the point $(0, j\,\Delta y - \Delta y/2)$

B be the point $(\varepsilon, j\,\Delta y - \Delta y/2)$

A' be the point $(0, j\,\Delta y + \Delta y/2)$

B' be the point $(\varepsilon, j\,\Delta y + \Delta y/2)$

where $0 < \varepsilon \ll \Delta y$.

Consider a constant velocity along BB' of magnitude $v_{0,j}^{(n)}$, and let the velocity component v be zero on the boundary AA' (Fig. 7). The circulation round $A\ B\ B'\ A'$ is $v_{0,j}^{(n)}\ \Delta y$ (neglecting the contributions from AB and $B'\ A'$ which are $0(\varepsilon)$). Further, the circulation round a square of side, Δy, is $\Delta y^2\omega$, where ω is the average vorticity in the square. Hence the vorticity at P is increased by:

$$\frac{v_{0,j}^{(n)}.\ \Delta y}{\Delta y^2} = \frac{v_{0,j}^{(u)}}{\Delta y}.$$

Therefore

$$\omega_{0,j}^{(n)} = \bar{\omega}_0(j\ \Delta y,\ n\Delta t) + \frac{v_{0,j}^{(n)}}{\Delta y}. \qquad .. \quad .. \quad .. \quad .. \quad (12)$$

where $\bar{\omega}_0(y,t)$ is the average of $\omega_0(Y,t)$ for $y - \Delta y/2 \leqslant Y \leqslant y + \Delta y/2$, and where $\omega_0(y,t) = -\{\partial u_0(y,t)/\partial y\}$.

2.6. *Method.*—Suppose ω and u,v are known at time, t, at all points $k \geqslant 0$, $-\infty < j < \infty$. Using equation (7) we can find ω at time $t + \Delta t$ at all points $k \geqslant 1$, $-\infty < j < \infty$. The velocity components u,v at time $t + \Delta t$ may then be found from equation (11) at all points $k \geqslant 0$, $-\infty < j < \infty$, and finally from equation (12) we obtain the vorticity, ω, at the boundary at points $k = 0$, $-\infty < j < \infty$.

Hence if ω and u,v are given at $t = 0$ for all x,y (the fluid was assumed to be initially at rest: $\omega = u = v = 0$ at $t = 0$) and $u_0(y,t)$ is given for all y and for $t \geqslant 0$, then ω and u,v can be calculated for all x,y and all $t > 0$.

2.7. *Improved Finite-Difference Approximations.*—(*a*) It was found that the use of the above finite-difference scheme gave satisfactory results only at very low Reynolds number, with the critical Reynolds number between 10 and 100. This was due to the instability of the finite difference equations which will be discussed in section 4.2. In order to get results for a higher Reynolds number the following modification was introduced.

In equation (7), $u_{K,J}^{(n)}$ and $v_{K,J}^{(n)}$ are functions of $\omega_{p,q}^{(n)}$ given by equations (11),

i.e.,

$$u_{K,J}^{(n)} = u_{K,J}(\omega_{p,q}^{(n)}),$$

$$v_{K,J}^{(n)} = v_{K,J}(\omega_{p,q}^{(n)}),$$

where p, q take all values such that $\omega_{p,q}^{(u)} \neq 0$ and $p \geqslant 1$.
Equation (7) is replaced by:

$$2\omega_{k,j}^{(n+1)} = \omega_{k,j}^{(n)} + \Omega_{k,j}^{(n+1)} + f\{u_{K,J}\ (\Omega_{p,q}^{(n+1)})\ ,\ v_{K,J}\ (\Omega_{p,q}^{(n+1)}),\ \Omega_{K,J}^{(n+1)}\} \quad .. \quad .. \quad (13)$$

where

$$\Omega_{k,j}^{(n+1)} = \omega_{k,j}^{(n)} + f\{u_{K,J}(\Omega_{p,q}^{(n)}),\ v_{K,J}(\Omega_{p,q}^{(n)}),\ \omega_{K,J}^{(u)}\}. \qquad .. \quad .. \quad .. \quad (14)$$

$\Omega_{k,j}^{(n+1)}$ is a first approximation to $\omega_{k,j}^{(n+1)}$ (and is usually also a good approximation).

(*b*) For a symmetrical jet $v\omega$ is an even function of y and since $v = \omega = 0$ when $y = 0$, $v\omega = 0(y^2)$ for small y. Hence at points such that $j = 1$, possible approximations for $-\Delta t\{\partial(v\omega)/\partial y\}$ are:

$$A = -\frac{\Delta t}{2\Delta x}\ (v_{k,2}^{(n)}\ \omega_{k,2}^{(n)} - v_{k,0}^{(n)}\ \omega_{k,0}^{(n)}) \quad .. \quad .. \quad .. \quad .. \quad .. \quad .. \quad (15)$$

$$B = -\frac{2\Delta t}{\Delta x}\ (v_{k,1}^{(n)}\ \omega_{k,1}^{(n)}) \qquad .. \quad .. \quad .. \quad .. \quad .. \quad .. \quad .. \quad (16)$$

and

$$C = -\frac{\Delta t}{6\Delta x}\ (v_{k,2}^{(n)}\ \omega_{k,2}^{(n)} + 8v_{k,1}^{(n)}\ \omega_{k,1}^{(n)})\ . \qquad .. \quad .. \quad .. \quad .. \quad .. \quad (17)$$

Equation (15) is the central difference formula of equations (6). Equation (16) is obtained by assuming $v\omega = \alpha y^2$ where α = constant. Equation (17) is obtained by assuming $v\omega = \alpha y^2 + \beta y^4$ where α = constant, β = constant. A, B and C were calculated at $t = 0{\cdot}45$ for Reynolds numbers 50 and 100 (The variation of the curved mesh width with j was neglected and $h_{k,j}\,\Delta = \frac{1}{4}$ was taken (*see* section 6)). Except for $k \leqslant 5$ for Reynolds number 50, A was much smaller in magnitude than either B or C, which both use the fact that $v\omega = \partial(v\omega)/\partial y = 0$ for $y = 0$. Since it was intended also to use the method for an unsymmetrical jet, in which case approximations B and C would not be valid, it was decided to use instead:

$$D_j = -\frac{2\Delta t}{3\Delta x}\left(v^{(n)}_{k,j+1}\,\omega^{(n)}_{k,j+1} - v^{(n)}_{k,j-1}\,\omega^{(n)}_{k,j-1}\right) + \frac{\Delta t}{12\Delta x}\left(v^{(n)}_{k,j+2}\,\omega^{(n)}_{k,j+2} - v^{(n)}_{k,j-2}\,\omega^{(n)}_{k,j-2}\right) \quad .. \quad .. \quad .. \quad .. \quad (18)$$

for all j. For $j = 1$ this was also calculated. It was seen that D_1 was larger than A but smaller than B or C (except for $k \leqslant 5$, $R = 50$, when all four expressions were of the same order of magnitude anyway).

Further, the truncation errors introduced by using the central difference for the y derivative and by using D_j have been calculated neglecting terms of order Δx^4. Although the use of D_j reduced the average size of the calculated errors, the values of B and C showed that the actual truncation errors for the v term at the points $j = 1$ are probably larger than the values calculated.

3. *Practical Details.*—3.1. *Procedure.*—The calculation was done with the aid of the Manchester University Mark I Electronic Computer. The constant coefficients $A_{a,b}$, $C_{k,j,l}$, $D_{a,b}$, $F_{k,j,l}$, (section 2.4) which were used repeatedly in the calculations of velocities, were first evaluated and kept permanently in the slow-speed magnetic drum store. They were also obtained on punched paper tape and could be quickly ' written ' into the store at the beginning of a run.

To simplify the programme of instructions for the computer, it was convenient to consider a fixed number of mesh points across the jet. Because of the size and arrangement of the stores (section 6.5), eleven points across the jet ($l_0 = 5$) were used throughout. Vorticity which spread beyond the outside points was neglected.

3.2. *Computing Time Involved.*—The problem has now been reduced to a series of multiplications and additions only, involving no divisions at all (The Manchester University Computer has no single instruction for division, this operation being performed by a series of multiplications and additions and several standard ' library routines ' are available to do this). The comparatively long time taken to do a division is thus avoided.

Each step in the integration may be divided into 5 stages. These are the evaluation of:

(*a*) $\Omega^{(n+1)}_{k,j}\ k \geqslant 1$ (equation (14))

(*b*) velocity (equations (11))

(*c*) $\Omega^{(n+1)}_{0,j}$ (equation (12) with $v^{(n+1)}_{0,j} = v_{0,j}\,(\Omega^{(n+1)}_{p,q})$)

(*d*) $\omega^{(n+1)}_{k,j}\ k \geqslant 1$ (equation (13))

(*e*) $\omega^{(n+1)}_{0,j}$, (equation (12) with $v^{(n+1)}_{0,j} = v_{0,j}\,(\omega^{(n+1)}_{q,q})$).

Most of the time taken by the computer was spent in stage (*b*); more precisely, in summing the series in the velocities which involve the vorticity (equations (8)). For a particular value of k, the velocity was found simultaneously for all eleven values of j.

In the calculations of the velocity at any point, regions of the half-plane where $\omega = 0$ need not be included since they make zero contribution to the velocity. Moreover it is unnecessary to go through stages (*a*) and (*d*) for points in these regions, as these equations merely show that ω remains zero at time $t + \Delta t$ (except that the region of non-zero vorticity may extend by at most two mesh lengths, one in stage (*a*) and one in stage (*d*)). Hence it is also unnecessary to calculate the velocity at points in a region of the half-plane where $\omega = 0$.

Now for a flow started from rest, the vorticity is everywhere zero at $t = 0$. Also vorticity cannot originate in the interior of the fluid but must be diffused or convected in from the boundary (Lamb, p. 578). Hence as t increases not only will more points be considered to calculate the velocity at any particular point, but also the velocity will be required at an incresing number of points. More precisely, the value of m_0 in equations (11) increases each step by at most 2 (but usually by 1 or 0; in no case did m_0 decrease) and the velocity is calculated only for points such that $k \leqslant m_0 + 2$.

For each value of m, $\omega_{m,l}^{(n)}$ were multiplied by $A_{k-m,j-l}$, etc., which alone involved 484 multiplications (using the curved mesh there was an additional series of terms in each of equations (8) (*see* section 6.3)), to do which the computer obeyed 2598 instructions (the additional instructions involved counting j and l, adding the partial sums into the accumulator and depositing the partial sums in the high speed store: this was done in the high-speed electronic store without reference to the magnetic drum store) and took 4 seconds. The time taken for a complete velocity was approximately $2 \cdot m_0 (m_0 + 2)$ times this which for $m_0 = 30$ amounted to 2 hours.

3.3. *Time-saving Approximations.*—It was therefore desirable that the instructions involved in the multiplying of $\omega_{m,l}^{(n)}$ by $A_{k-m,j-l}$, etc., should be as few as possible.

Most instructions involving the accumulator (certainly addition and multiplication instructions) are concerned with numbers in long lines of 40 binary digits. Since short line numbers were being used the 20 least significant digits of the corresponding long line were made zero before the number was used, in order to avoid large round-off errors (*see* section 4.3). The short lines had previously been rounded off to 20 digits.

In this part of the calculation this procedure was not followed, long lines being used for $A_{a,b}$, $B_{a,b}$, $D_{a,b}$ and $E_{a,b}$ (*see* section 6.3) with the number in the 20 least significant digits unaltered (As well as being rounded off to 20 digits, 1 was subtracted from the 20th digit if the 21st significant digit of the corresponding long line would be 1). In this way the time taken to evaluate the velocity was kept to a minimum.

If the velocity changes by only a small amount in the time Δt of the step in the integration, it is possible to omit the velocity calculation, using the velocity of the previous step in stage (*d*) and also in stage (*a*) of the next step, without introducing a larger error. The velocity at the entry, $u_0(y,t)$ was (for given y) increased from zero at $t = 0$ to a maximum at which it was kept constant. Hence the velocity at any point will tend to a constant value as t increases (assuming that a steady flow will be ultimately obtained in this way) so that this device can be used to shorten the calculation.

In order to decide when the error involved was sufficiently small to make this simplification, the error was estimated as follows. When the velocity had been calculated at a set of points $k = k_1$, $-5 \leqslant j \leqslant 5$, and before it was written into the magnetic drum store, an integration similar to stage (*a*) was carried out twice for these points:

(i) using the velocity already in the magnetic drum store, which had been calculated in a previous step in the integration

(ii) using the velocity just calculated.

(To do this a difference equation corresponding to equation (1):

$$\frac{\partial \omega}{\partial t} = u \frac{\partial \omega}{\partial x} + v \frac{\partial \omega}{\partial y} + \nu \left(\frac{\partial^2 \omega}{\partial x^2} + \frac{\partial^2 \omega}{\partial y^2} \right),$$

was used. For a particular point only one velocity is involved, the velocity at that point.) The maximum for all points of the field of the difference between the two values of $\Omega_{k,j}^{(n+1)}$ so obtained for each point is approximately the maximum error in the vorticity that would have been introduced if the velocity calculation had been omitted in that step. Let this maximum difference be E, and suppose the velocity is being evaluated every sth step, having last been evaluated in the n_0th step. Then E is the maximum error introduced in the $(n_0 + s)$th step by using the n_0th velocity instead of the $(n_0 + s)$th velocity (Actually the error in stage (d) of the $(n_0 + s)$ step is $\frac{1}{2}E$ and in stage (a) of the $(n_0 + s + 1)$th step is also $\frac{1}{2}E$). Assuming the error to be proportional to the number of times the velocity calculation has been omitted, the maximum error introduced in the $(n_0 + p)$th step is $(p/s)E$. Therefore the inherited error in the $(n_0 + 2s)$th step due to the $(2s)$ steps performed without evaluating the velocity is:

$$\sum_{p=1}^{2s} \frac{p}{s} E = (2s + 1)E.$$

(This would also be obtained by assuming E to be the average error introduced in the n_0th to the $(n_0 + 2s)$th steps inclusive). If $(2s + 1)E < 4$ per cent of the average vorticity at the orifice $(= 50)$, the velocity was evaluated only in every $2s$th step from then on. In this way the error introduced in a number of consecutive steps in which the velocity is not calculated is below 4 per cent at every point.

4. *Stability and Errors.*—4.1. *Stability of Difference Equations.*—Several investigations have been made of the accuracy of the numerical integration of differential equations by finite-difference methods. Because of inconsistency of nomenclature, I shall redefine the terms used. suppose D is the exact solution of the differential equation, together with the given initial and boundary conditions, and let E and N be the exact and numerical solutions of the difference equation, together with the given initial and boundary conditions.

Definition 1
$|D - N|$ is the ' total error '

Definition 2
$|E - D|$ is the ' truncation error '

Definition 3
$|E - N|$ is the ' numerical error '

Definition 4
If $|E - D| \to 0$ as the mesh widths $\to 0$ in a suitable manner, the difference equation is ' convergent '

Definition 5
If $|N - E|$, the numerical error, is small throughout the entire region of integration, the finite difference equation is ' stable '

Definition 6
If there exists a constant $K > 0$ such that $|E| < K$ throughout the entire region, the difference equation is ' bounded '.

The numerical error is usually considered to consist of the inherited aggregate of round-off errors. The question of whether the round-off errors introduced in a particular step will increase in subsequent steps is closely related to the question of whether the solution of the difference equation is bounded. F. John defines stability by definition 6, which is here termed boundedness, a word which is not commonly used in the literature.

Since with low viscosity (high Reynolds number) hydrodynamical instability, leading to turbulence, quickly sets in, one can expect a numerical method to become unsatisfactory at high Reynolds number. In section 4.2 a condition necessary both for stability and boundedness is deduced. This condition relates the Reynolds number based on the mesh width to the time interval.

4.2. *The von Neumann-Ritchmyer Technique.*—Consider the differential equation (3):

$$\frac{\partial \omega}{\partial t} + \frac{\partial (u\omega)}{\partial x} + \frac{\partial (v\omega)}{\partial y} = \nu\left(\frac{\partial^2 \omega}{\partial x^2} + \frac{\partial^2 \omega}{\partial y^2}\right).$$

Suppose that in a region $\mathscr{R}$, u = constant, v = constant. Let $L = u\,\Delta t/2\Delta x$, $N = v\,\Delta t/2\Delta x$, $M = v\,\Delta t/\Delta x^2$.

(*a*) Consider the finite-difference equation (7) which can be written:

$$\omega_{k,j}^{(n+1)} = \omega_{k,j}^{(n)} + L(\omega_{k-1,j}^{(n)} - \omega_{k+1,j}^{(n)}) + N(\omega_{k,j-1}^{(n)} - \omega_{k,j+1}^{(n)})$$
$$+ M(\omega_{k+1,j}^{(n)} + \omega_{k-1,j}^{(n)} + \omega_{k,j+1}^{(n)} + \omega_{k,j-1}^{(n)} - 4\omega_{k,j}^{(n)}). \quad .. \quad .. \quad .. \quad (19)$$

Following von Neumann and Ritchmyer, let us seek a solution of (19) of the form:

$$\omega_{k,j}^{(n)} = g(t)\, e^{i\theta x} e^{i\phi y} \quad .. \quad .. \quad .. \quad .. \quad .. \quad .. \quad (20)$$

where $x = k\,\Delta x$, $y = j\,\Delta y$, $t = n\,\Delta t$, and where θ and ϕ are constants. This solution is:

$$\omega_{k,j}^{(n)} = \{1 + f(\theta\,\Delta x, \phi\,\Delta y)\}^n e^{i\theta x} e^{i\phi y}, \quad .. \quad .. \quad .. \quad .. \quad (21)$$

where

$$\omega_{k,j}^{(0)} = e^{i\theta x} e^{i\phi y}, \quad .. \quad .. \quad .. \quad .. \quad .. \quad .. \quad .. \quad (22)$$

and where

$$\left.\begin{aligned} f(\theta,\phi) &= (L + M)\, e^{-i\theta} - (L - M)\, e^{i\theta} \\ &\quad + (N + M)\, e^{-i\theta} - (N - M)\, e^{i\phi} - 4M \\ &= -4M + 2M\cos\theta + 2M\cos\phi \\ &\quad - 2i(L\sin\theta + N\sin\phi) \end{aligned}\right\} .. \quad .. \quad (23)$$

Let Δt, Δx, $\Delta y \to 0$, k, j and n passing through integral values.

$$\omega_{k,j}^{(n)} \to e^{-\nu(\theta^2 + \phi^2)t}\, e^{-i(\theta u + \phi v)t}\, e^{i(\theta x + \phi y)} \quad .. \quad .. \quad .. \quad .. \quad (24)$$
$$= \omega(x,y,t), \text{ say,}$$

which is easily seen to be the solution of the differential equation (3), with the initial condition, $\omega(x,y,0) = e^{i\theta x} e^{i\phi y}$.

Since any initial value of ω, $\omega_{k,j}^{(0)}$, can be expressed as a linear combination of terms such as (22) by Harmanic analysis (only a finite area of the x-y plane is being considered here), the solution, $\omega_{k,j}^{(n)}$, of the difference equation is a linear combination of terms such as (21) (Since u = constant, v = constant, equation (19) is linear). Further, assuming the double integrals involved are uniformly convergent as Δx, Δy, $\Delta t \to 0$, $\omega_{k,j}^{(n)} \to \omega(x,y,t)$, where $\omega(x,y,t)$ is the solution of the differential equation (3). Therefore the difference equation (19) is convergent.

However, the difference equation (19) is not bounded for certain values of Δx, Δy and Δt, as the solution (21) of the difference equation may be such that $|\omega_{k,j}^{(n)}| \to \infty$ as $n \to \infty$ (The corresponding solution, (24), of the differential equation tends to zero as $t \to \infty$, except when $\theta = \phi = 0$ when it is a constant). A necessary condition for boundedness of the difference equation is that $\omega_{k,j}^{(n)}$ given by (21) is bounded as $t \to \infty$, which is so if:

$$|1 + f(\theta, \phi)| \leqslant 1 \quad .. \quad .. \quad .. \quad .. \quad .. \quad (25)$$

for all θ, ϕ such that $|\theta| < \pi$, $|\phi| < \pi$ (This is the extension to two space co-ordinates of F. John's ' necessary condition for stability ').

The numerical error introduced for $t \leqslant 0$ will satisfy the same equation as $\omega_{k,j}^{(n)}$ (equation (19)), and analysing the error at $t = 0$ into Fourier components, we also obtain (25) as a necessary condition for stability.

Let
$$g(\theta, \phi) = |1 + f(\theta, \phi)|^2$$
$$= (1 - 4M + 2M\cos\theta + 2M\cos\phi)^2 + 4(L\sin\theta + N\sin\phi)^2. \quad . . \quad (26)$$

Therefore when $\theta = \phi = 0$, $g = 1$, $\partial g/\partial\theta = 0$, $\partial^2 g/\partial\theta^2 = -4M + 8L^2$.

Therefore, if condition (25) is to be satisfied:

$$M \geqslant 2L^2 \quad . . \quad . . \quad . . \quad . . \quad . . \quad (27)$$

is necessary.

Let
$$R_m = \frac{8|L|}{M}$$
$$= \frac{4|u|\Delta x}{\nu}$$
$$= 4 \times \text{the Reynolds number based on the mesh width.}$$

$$R_m \leqslant \frac{4}{|L|} \quad . . \quad . . \quad . . \quad . . \quad . . \quad (28)$$

is a necessary condition for stability and boundedness (*see* Graph 20a). Also $g(\pi/2, 0) \leqslant 1$ can be satisfied only if:

$$|L| \leqslant \tfrac{1}{2}, \quad . . \quad . . \quad . . \quad . . \quad . . \quad (29)$$

which is the Courant-Friedrichs-Lewy condition for stability when $M = N = 0$, and $g(\pi/2, \pi/2) \leqslant 1$ can be satisfied only if:

$$M \leqslant \tfrac{1}{2}, \quad . . \quad . . \quad . . \quad . . \quad . . \quad (30)$$

which is the Courant-Friedrichs-Lewy condition for stability for a simple finite-difference approximation to the heat equation ($L = N = 0$). (29) and (30) are further necessary conditions for stability and boundedness.

Using this finite-difference scheme the results for Reynolds number 100 showed oscillations, rapidly increasing in amplitude as t increases, as would be expected from this investigation of stability (For the curved mesh of Section 6 which was used to obtain the results, the region $\mathscr{R}$ is such that $h_{k,j}$ is almost constant in $\mathscr{R}$ and

$$L = \frac{U\,\Delta t}{2h\,\Delta}, \; N = \frac{V\,\Delta t}{2h\,\Delta}, \; M = \frac{\nu\,\Delta t}{h^2\Delta^2}).$$

For Reynolds number 10, the equation was stable and bounded, no oscillations appearing in the results at all. However, vorticity spread away from the axis of symmetry and so the curved mesh did not cover the region of large vorticity.

(*b*) Consider the difference equation:

$$\omega_{k,j}^{n+1} = \omega_{k,j}^{n-1} + 2L(\omega_{k-1,j}^{(n)} - \omega_{k+1,j}^{(n)}) + 2N(\omega_{k,j-1}^{(n)} - \omega_{k,j+1}^{(n)})$$
$$+ 2M(\omega_{k+1,j}^{(n)} + \omega_{k-1,j}^{(n)} + \omega_{k,j+1}^{(n)} + \omega_{k,j-1}^{(n)} - 4\omega_{k,j}^{(n)}) \quad . . \quad . . \quad (31)$$

obtained by using the central time difference, $(\omega_{k,j}^{(n+1)} - \omega_{k,j}^{(n-1)})/2\Delta t$. A similar analysis shows that equation (31) is unstable and unbounded for any values of Δx and Δt.

No attempt was made to obtain results using this difference equation.

(*c*) Consider the difference equation:

$$2w_{k,j}^{(n+1)} = \omega_{k,j}^{(n)} + \Omega_{k,j}^{(n+1)} + L(\Omega_{k-1,j}^{(n+1)} - \Omega_{k+1,j}^{(n+1)}) + N(\Omega_{k,j-1}^{(n+1)} - \Omega_{k,j+1}^{(n+1)})$$
$$+ M(\Omega_{k+1,j}^{(n+1)} + \Omega_{k-1,j}^{(n+1)} + \Omega_{k,j+1}^{(n+1)} + \Omega_{k,j-1}^{(n+1)} - 4\Omega_{k,j}^{(n+1)}) \quad .. \quad .. \quad (32)$$

in which

$$\Omega_{k,j}^{(n+1)} = \omega_{k,j}^{(n)} + L(\omega_{k-1,j}^{(n)} - \omega_{k+1,j}^{(n)}) + N(\omega_{k,j-1}^{(n)} - \omega_{k,j+1}^{(n)})$$
$$+ M(\omega_{k+1,j}^{(n)} + \omega_{k-1,j}^{(n)} + \omega_{k,j+1}^{(n)} + \omega_{k,j-1}^{(n)} - 4\omega_{k,j}^{(n)}),$$

obtained by using the improved finite-difference approximation for the t derivative described in section 2.7. Again let us seek a solution of the form (20). We must have:

$$2\omega_{k,j}^{(n+1)} = \omega_{k,j}^{(n)} + \{1 + f(\theta\,\Delta x, \phi\,\Delta y)\}\Omega_{k,j}^{(n+1)}$$

and

$$\Omega_{k,j}^{(n+1)} = \{1 + f(\theta\,\Delta x, \phi\,\Delta y)\}\omega_{k,j}^{(n)}.$$

Therefore

$$\omega_{k,j}^{(n)} = \left[\frac{1 + \{1 + f(\theta\,\Delta x, \phi\,\Delta y)\}^2}{2}\right]^n e^{i\theta x}\, e^{i\phi y}.$$

As before, a necessary condition for stability and boundedness is:

$$g_1(\theta, \phi) = |1 + \{1 + f(\theta, \phi)\}^2|^2 \leqslant 4 \quad .. \quad .. \quad .. \quad .. \quad .. \quad .. \quad (33)$$

for all θ, ϕ such that $|\theta| < \pi, |\phi| < \pi$.

$$g_1(\theta, \phi) = \{1 + (1 - 4M + 2M\cos\theta + 2M\cos\phi)^2 - 4(L\sin\theta + N\sin\phi)^2\}^2$$
$$+ 16\,(1 - 4M + 2M\cos\theta + 2M\cos\phi)^2\,(L\sin\theta + N\sin\phi)^2.$$

$$g_1(\theta, 0) = \{1 + (1 - Y)^2 - 4X^2\}^2 + 16\,(1 - Y)^2\,X^2$$
$$= \{1 + (1 - Y)^2 + 4X^2\}^2 - 16X^2.$$

where

$$X = |L|\sin\theta$$
$$Y = 2M(1 - \cos\theta).$$

If $g_1(\theta, 0) \leqslant 4$, then:

$$(1 - Y)^2 \leqslant 2\sqrt{(1 + 4X^2)} - (1 + 4X^2) \quad .. \quad .. \quad .. \quad (34)$$

is necessary.

Therefore $Y \geqslant 1 - \{2\sqrt{(1 + 4X^2)} - (1 + 4X^2)\}^{1/2}$ is necessary.

Let

$$h(X) = 16X[1 - \{2\sqrt{(1 + 4X^2)} - (1 + 4X^2)\}^{1/2}]^{-1} \quad .. \quad .. \quad (35)$$

and let

$$(R^m)_{\text{critical}} = \overset{\text{minimum}}{|\theta| < \pi}\left\{\frac{1 - \cos\theta}{\sin\theta}\, h(|L|\sin\theta)\right\}. \quad .. \quad .. \quad .. \quad .. \quad (36)$$

Then a necessary condition for stability and boundedness is:

$$R_m \leqslant (R_m)_{\text{critical}}.$$

$$\frac{d}{d\theta}\left\{\frac{1-\cos\theta}{\sin\theta}\,h(|L|\sin\theta)\right\}$$

$$= (-\operatorname{cosec}\theta\cot\theta + \operatorname{cosec}^2\theta)h(|L|\sin\theta)$$

$$+\frac{1-\cos\theta}{\sin\theta}\,h'(|L|\sin\theta)\,|L|\cos\theta$$

$$=\frac{1-\cos\theta}{\sin^2\theta}\{h(X)+\cos\theta\,h'(X)\}.$$

For $X > 0$, $h(X) > 0$ and from the graph of $h(X)$ (Graph 20c), we see that $h'(X) < 0$.

Therefore: $$\frac{d}{d\theta}\left\{\frac{1-\cos\theta}{\sin\theta}\,h(X)\right\} \geqslant 0$$

for $\pi/2 < \theta < \pi$.

Therefore: $\dfrac{1-\cos\theta}{\sin\theta}\,h(X)$ is a minimum for θ such that:

$$\cos\theta = \frac{h(X)}{X(-h'(X))}.$$

$h'(X)$ was obtained by measuring the slope of the graph of $h(X)$ and hence the value of θ for the minimum and the graph of $(R_m)_{\text{critical}}$ against L were obtained (Graph 20b).

There is also a lower bound to R_m necessary for stability. Such a condition may be obtained from equation (34) for $Y > 1$. More simply, a necessary condition for stability and boundedness is $g_1(\pi, \pi) \leqslant 4$, *i.e.*, $\{1 + (1 - 8M)^{\frac{1}{2}}\}^2 \leqslant 4$. Therefore $M \leqslant \frac{1}{4}$. Therefore $R_m \geqslant 32\,|L|$ is also necessary for stability and boundedness (Graph 20d).

4.3. *Truncation Errors.*—Consider a rectangular mesh with $\Delta x = \Delta y$.

Let $\bar{f}(x,y,t)$

$$= \frac{1}{\Delta x^2}\int_{x-(\Delta x/2)}^{x+(\Delta x/2)}\int_{y-(\Delta y/2)}^{y+(\Delta y/2)} f(X,Y,t)\,dX\,dY$$

$$=\text{the average of } f(X,Y,t) \text{ for}$$

$$x - \frac{\Delta x}{2} \leqslant X \leqslant x + \frac{\Delta x}{2}$$

$$y - \frac{\Delta y}{2} \leqslant Y \leqslant y + \frac{\Delta y}{2} \qquad (37)$$

Let $\omega(x,y,t)$ be the solution for $t \geqslant n\,\Delta t$ of the differential equations (2) and (3) such that $\omega(x,y,n\,\Delta t) = \omega_0(x,y,n\,\Delta t)$ is given and with the boundary conditions $u(o,y,t) = u_0(y,t)$ and $v(o,y,t) = 0$. Taking the average of each term in equation (3) and interchanging the orders of

Also

$$\bar{u}(x+\Delta x,y,t)\bar{\omega}(x+\Delta x,y,t) - \bar{u}(x-\Delta x,y,t)\bar{\omega}(x-\Delta x,y,t)$$

$$= 2\Delta x(\bar{u}\bar{\omega})_x + \frac{\Delta x^3}{3}(\bar{u}\bar{\omega})_{xxx} + 0(\Delta x^5)$$

$$= 2\Delta x\left\{u_x + \frac{\Delta x^2}{24}(u_{xx}+u_{yy})_x\right\}\left\{\omega + \frac{\Delta x^2}{24}(\omega_{xx}+\omega_{yy})\right\}$$

$$- 2\Delta x\left\{u + \frac{\Delta x^2}{24}(u_{xx}+u_{yy})\right\}\left\{\omega_x + \frac{\Delta x^2}{24}(\omega_{xx}+\omega_{yy})_x\right\}$$

$$+ \frac{\Delta x^3}{3}\left\{u_{xxx}\,w + 3u_{xx}\,\omega_x + 3u_x\,\omega_{xx} + u\omega_{xxx}\right\} + 0(\Delta x^5)$$

$$= 2\Delta x\,(u\omega)_x + \frac{\Delta x^3}{12}\left[4(u\omega)_{xxx} + \{(u_{xx}+u_{yy})\omega + u(\omega_{xx}+\omega_{yy})\}_x\right] + 0(\Delta x^5).$$

Therefore:

$$(E_t)_{k,j}^{(n+1)} = -\frac{\Delta t^2}{2}\left(\frac{\partial^2\bar{\omega}}{\partial t^2}\right)_{k,j}^{(n)} - \frac{\Delta t^3}{6}\left(\frac{\partial^3\bar{\omega}}{\partial t^3}\right) + 0(\Delta t^4)$$

$$= -\frac{1}{6}(\omega_{k,j}^{(n+2)} - 3\omega_{k,j}^{(n)} + 2\omega_{k,j}^{(n-1)}) + 0(\Delta t^4)$$

$$(E_u)_{k,j}^{(n+1)} = \frac{\Delta t\,\Delta x^2}{24}\left[-3(u\omega)_{xxx} + (u\omega)_{xyy} - \{(u_{xx}+u_{yy})\omega\right.$$

$$\left. + u(\omega_{xx}+\omega_{yy})\}_x\right] + 0(\Delta x^4)$$

$$(E_v)_{k,j}^{(n+1)} = \frac{\Delta t\,\Delta x^2}{24}\left[-3(v\omega)_{yyy} + (v\omega)_{xxy} - \{(v_{xx}+v_{yy})\omega\right.$$

$$\left. + v(\omega_{xx}+\omega_{yy})\}_y\right] + 0(\Delta x^4).$$

Since

$$v_x - u_y = \omega,$$

$$u_x + v_y = 0,$$

we have

$$u_{xx} + u_{yy} = -\omega_y,$$

$$v_{xx} + v_{yy} = +\omega_x.$$

Therefore:

$$(E_u + E_v)_{k,j}^{(n+1)} = \frac{\Delta t\,\Delta x^2}{24}\left\{-3(u\omega)_{xxx} - 3(v\omega)_{yyy} + (u\omega)_{xyy} + (v\omega)_{xxy}\right.$$

$$\left. - u(\omega_{xx}+\omega_{yy})_x - v(\omega_{xx}+\omega_{yy})_y\right\} + 0(\Delta x)^4.$$

Since only $E_u + E_v$ is required, it will be sufficient to take:

$$(E_u)_{k,j}^{(n+1)} = \frac{\Delta t\,\Delta x^2}{24}\left\{-3(u\omega)_{xxx} + (u\omega)_{xyy} - u(\omega_{xx}+\omega_{yy})_x\right\} + 0(\Delta x^4)$$

$$= \frac{\Delta t\,\Delta x^2}{24}\left\{-3(\bar{u}\bar{\omega})_{xxx} + (\bar{u}\bar{\omega})_{xyy} - \bar{u}(\bar{\omega}_{xx} + \bar{\omega}_{yy})_x\right\} + 0(\Delta x^4)$$

$$= \frac{\Delta t}{48\Delta x}\left\{-3\left[\bar{u}\bar{\omega}^{(n)}_{k+2,j} - 2(\bar{u}\bar{\omega})^{(n)}_{k+1,j} + 2(\bar{u}\bar{\omega})^{(n)}_{k-1,j} - (\bar{u}\bar{\omega})^{(n)}_{k-2,j}\right]\right.$$

$$+\left[(\bar{u}\bar{\omega})^{(n)}_{k+1,j+1} - 2(\bar{u}\bar{\omega})^{(m)}_{k+1,j} + (\bar{u}\bar{\omega})^{(n)}_{k+1,j-1} - (\bar{u}\bar{\omega})^{(n)}_{k-1,j+1}\right.$$

$$\left.+\,2(\overline{u\omega})^{(n)}_{k-1,j} - (\overline{u\omega})^{(n)}_{k-1,j-1}\right]$$

$$-\bar{u}^{(n)}_{k,j}\left[\bar{\omega}^{(n)}_{k+2,j} + \bar{\omega}^{(n)}_{k+1j+1} - 4\bar{\omega}^{(n)}_{k+1,j} + \bar{\omega}^{(n)}_{k+1,j-1} - \bar{\omega}^{(n)}_{k-2,j}\right.$$

$$\left.\left.-\,\bar{\omega}^{(n)}_{k-1,j+1} + 4\bar{\omega}^{(n)}_{k-1,j} - \bar{\omega}^{(n)}_{k-1,j-1}\right]\right\} + 0(\Delta x^4) \quad .. \quad .. \quad .. \quad (38)$$

and

$$(E_v)^{(n+1)}_{k,j} = \frac{\Delta t}{48\Delta x}\left\{-3\left[(\bar{v}\bar{\omega})^{(n)}_{k,j+2} - 2(\bar{v}\bar{\omega})^{(n)}_{k,j+1} + 2(\bar{v}\bar{\omega})^{(n)}_{k,j-1} - (\bar{v}\bar{\omega})^{(n)}_{k,j-2}\right]\right.$$

$$+\left[(\bar{v}\bar{\omega})^{(n)}_{k+1,j+1} - 2(\bar{v}\bar{\omega})^{(n)}_{k,j+1} + (\bar{v}\bar{\omega})^{(n)}_{k-1,j+1} - (\bar{v}\bar{\omega})^{(n)}_{k+1,j-1}\right.$$

$$\left.+\,2(\bar{v}\bar{\omega})^{(n)}_{k,j-1} - (\bar{v}\bar{\omega})^{(n)}_{k-1,j-1}\right]$$

$$-\bar{v}^{(n)}_{k,j}\left[\bar{\omega}^{(n)}_{k,j+2} + \bar{\omega}^{(n)}_{k+1,j+1} - 4\bar{\omega}^{(n)}_{k,j+1} + \bar{\omega}^{(n)}_{k-1,j+1}\right.$$

$$\left.\left.-\,\bar{\omega}^{(n)}_{k,j-2} - \bar{\omega}^{(n)}_{k+1,j-1} + 4\bar{\omega}^{(n)}_{k,j-1} - \bar{\omega}^{(n)}_{k-1,j-1}\right]\right\} + 0(\Delta x^4) \quad .. \quad (39)$$

$$(E_d)^{(n+1)}_{k,j} = \frac{\nu\,\Delta t\,\Delta x^2}{12}(\bar{\omega}_{xxxx} + \bar{\omega}_{yyyy}) + 0(\Delta x^4)$$

$$= \frac{\nu\,\Delta t}{12\Delta x^2}\left\{\bar{\omega}^{(n)}_{k+2,j} - 4\bar{\omega}^{(n)}_{k+1,j} + \bar{\omega}^{(n)}_{k,j+2} - 4\bar{\omega}^{(n)}_{k,j+1} + 12\bar{\omega}^{(n)}_{k,j}\right.$$

$$\left.-\,4\bar{\omega}^{(n)}_{k,j-1} + \bar{\omega}^{(n)}_{k,j-2} - 4\bar{\omega}^{(n)}_{k-1,j} + \bar{\omega}^{(n)}_{k-2,j}\right\} + 0(\Delta x^4).$$

Let E_t' and E_v' be the corresponding errors using the improved approximations for the t derivative and y derivative (section 2.7) and let $E' = E_t' + E_u + E_v' + E_d$. Neglecting the truncation errors in the space derivative the improved approximation for the t derivative gives, approximately:

$$\Omega^{(n+1)}_{k,j} = \bar{\omega}^{(n)}_{k,j} + \Delta t\left(\frac{\partial\bar{\omega}}{\partial t}\right)^{(n)}_{k,}$$

and

$$2Z^{(n+1)}_{k,j} = \bar{\omega}^{(n)}_{k,j} + \Omega^{(n+1)}_{k,j} + \Delta t\left(\frac{\partial}{\partial t}\left[\bar{\omega} + \Delta t\,\frac{\partial\bar{\omega}}{\partial t}\right]\right)^{(n)}_{k,j}.$$

Therefore:

$$Z^{(n+1)}_{k,j} = \bar{\omega}^{(n)}_{k,j} + \Delta t\left(\frac{\partial\bar{\omega}}{\partial t}\right)^{(n)}_{k,j} + \frac{\Delta t^2}{2}\left(\frac{\partial^2\bar{\omega}}{\partial t^2}\right)^{(n)}_{k,j}.$$

Therefore:

$$(E_t')_{k,j}^{(n+1)} = -\frac{\Delta t^3}{6}\left(\frac{\partial^3\bar{\omega}}{\partial t^3}\right)_{k,j}^{(n)} + 0(\Delta t^4)$$

$$= -\frac{1}{6}\left\{\bar{\omega}_{k,j}^{(n+2)} - 3\bar{\omega}_{k,j}^{(n+1)} + 3\bar{\omega}_{k,j}^{(n)} - \bar{\omega}_{k,j}^{(n-1)}\right\} + 0(\Delta t^4)\,.$$

The improved approximation for the y derivative is the approximation of $\partial(\overline{v\omega})/\partial y$ by:

$$\frac{2}{3\Delta x}\left\{(\bar{v}\bar{\omega})_{k,j+1}^{(n)} - (\bar{v}\bar{\omega})_{k,j-1}^{(n)}\right\} - \frac{1}{12\Delta x}\left\{(\bar{v}\bar{\omega})_{k,j+2}^{(n)} - (\bar{v}\bar{\omega})_{k,j-2}^{(n)}\right\}.$$

Therefore:

$$(E_v')_{k,j}^{(n+1)} = (E_v)_{k,j}^{(n+1)} + \frac{2}{3}\frac{\Delta t}{\Delta x}\left\{(\bar{v}\bar{\omega})_{k,j-1}^{(n)} - (\bar{v}\bar{\omega})_{k,j+1}^{(n)}\right\}$$

$$- \frac{1}{12}\frac{\Delta t}{\Delta x}\left\{(\bar{v}\bar{\omega})_{k,j-2}^{(n)} - (\bar{v}\bar{\omega})_{k,j+2}^{(n)}\right\} - \frac{\Delta t}{2\Delta x}\left\{(\bar{v}\bar{\omega})_{k,j-1}^{(n)} - (\bar{v}\bar{\omega})_{k,j+1}^{(n)}\right\}$$

(When the improved t derivative approximation is being used, the truncation error in the term, $-\{\partial(\overline{u\omega})/\partial x\}\Delta t$, is more accurately given by $\frac{1}{2}(E_u)_{k,j}^{(n+1)} + \frac{1}{2}(E_u)_{k,j}^{(n+2)}$. However, since $(E_u)_{k,j}^{(n+1)}$ and $(E_u)_{k,j}^{(n+2)}$ will be of the same order of magnitude, it is sufficient to take the error as $(E_u)_{k,j}^{(n+1)}$. Similarly $(E_v')_{k,j}^{(n+1)}$ and $(E_d)_{k,j}^{(n+1)}$ only are calculated).

E_t', $E_u + E_v'$, E_d and E' (and also $E_u + E_v$) were calculated for Reynolds number 50 at $t = 0{\cdot}45$. E', the truncation error introduced in the 46th step, is everywhere less than $0{\cdot}50$ which is 1 per cent of the average vorticity at the orifice. E_t' is negligible being nowhere greater than $0{\cdot}02$. E_d is positive at all points $j = 1$ and is also very large behind the front whirls. This truncation error is almost entirely due to the approximation of $\partial^2\bar{\omega}/\partial y^2$ by $(1/\Delta x^2)\ (\bar{\omega}_{k,j+1}^{(n)} - 2\bar{\omega}_{k,j}^{(n)} + \bar{\omega}_{k,j-1}^{(n)})$, so more accurate results could have been obtained for this Reynolds number by using a higher approximation for this derivative such as $(1/12\Delta x^2)\ (-\bar{\omega}_{k,j+2}^{(n)} - \bar{\omega}_{k,j-2}^{(n)} + 16\bar{\omega}_{k,j+1}^{(n)} + 16\bar{\omega}_{k,j-1}^{(n)} - 30\bar{\omega}_{k,j}^{(n)})$. For Reynolds number 100, the coefficient of viscosity is half that for Reynolds number 50, so that:

$$\frac{\text{maximum } |E_d|}{\text{maximum } |E_u + E_v'|}$$

for Reynolds number 100 would be roughly half that for Reynolds number 50. The reduction in the truncation error, E', would be less significant and would be negligible for Reynolds number 300.

The truncation errors have not been calculated for Reynolds number 100, 150, 300 since the large instability oscillations would far exceed the truncation errors.

4.4. *Other Sources of Error.*—(*a*) *Errors in the Velocity.*—(i) Error in the velocity due to the source flow (equation 10). This will be greatest near the orifice. At the point $(\Delta x, o)$ the velocity component u due to the source flow is:

$$u = \frac{1}{\pi}\int_{-\infty}^{\infty} u_0(y,t)\,\frac{\Delta x}{\Delta x^2 + y^2}\,dy \qquad \ldots\ \ldots\ \ldots\ \ldots\ \ldots\ \ldots \quad (40)$$

$$= \frac{2}{\pi}\int_0^{1/2} U\,\frac{3}{2}(1 - 4y^2)\,\frac{\frac{1}{4}}{\frac{1}{16} + y^2}\,dy$$

$$= \frac{3U}{4\pi}(5\tan^{-1}2 - 2)$$

$$= 13{\cdot}96.$$

If the integral (40) is calculated by the ' point sources ' method (equation (10) one obtains:

$$u = \frac{1}{\pi}\left\{\bar{u}_0(0,t) + 2\bar{u}_0(\Delta x,t).\,\tfrac{1}{2} + 2\bar{u}_0(2\Delta x,t).\,\frac{1}{5}\right\}$$

$$= 13{\cdot}82$$

which is small by $0{\cdot}8$ per cent of the average velocity, at the orifice, U.

(ii) The error in the velocity due to replacing the uniform vorticity, ω, in a square of side, Δx, by a point vortex of strength $\omega\Delta x^2$ at the centre.

Consider the velocity component v at the point $(\Delta x,0)$ due to a uniform distribution of vorticity, ω, in the square:

$$|x| \leqslant \frac{\Delta x}{2}$$

$$|y| \leqslant \frac{\Delta x}{2}.$$

It is given by

$$v = \int_{-\Delta x/2}^{\Delta x/2}\int_{-\Delta x/2}^{\Delta x/2} \frac{\omega\, dx\, dy}{2\pi R}\,\frac{\Delta x - x}{R}$$

where $$R^2 = (\Delta x - x)^2 + y^2.$$

Therefore

$$v = \frac{\omega}{2\pi}\left[y\log\left\{\frac{\left(\frac{3\Delta x}{2}\right)^2 + y^2}{\left(\frac{\Delta x}{2}\right)^2 + y^2}\right\} + 3\Delta x\tan^{-1}\frac{y}{3\Delta x/2} - \Delta x\tan^{-1}\frac{y}{\Delta x/2}\right]_{y=0}^{y=\Delta x/2}$$

$$= 0{\cdot}985\,\frac{\omega\,\Delta x}{2\pi}.$$

Therefore the error is $0{\cdot}015$ $(\omega\,\Delta x/2\pi)$ which for $\omega = 50$ is $0{\cdot}31$ which is $0{\cdot}2$ per cent of U.

(iii) For a non-uniform distribution of vorticity the error may be greater. Suppose:

$$\omega(x,y,n\,\Delta t) = \omega_{k,j}^{(n)} + (x - k\,\Delta x)\left(\frac{\partial\omega}{\partial x}\right)_{k,j}^{(n)} + (y - j\,\Delta y)\left(\frac{\partial\omega}{\partial y}\right)_{k,j}^{(n)}$$

for (x,y) in the square:

$$\left.\begin{aligned} |x - k\,\Delta x| &\leqslant \Delta x/2 \\ |y - j\,\Delta y| &\leqslant \Delta y/2 \end{aligned}\right\} \quad .. \quad .. \quad .. \quad .. \quad (41)$$

The velocity at the point $(k\,\Delta x,\, j\,\Delta y)$ due to this vorticity is given approximately by the sum of the effects of four point vortices, of strengths:

$$\omega_1 \text{ at the point } \left(k\,\Delta x + \frac{\Delta x}{2}\,,\, j\,\Delta x + \frac{\Delta x}{2}\right)$$

which means that:

$\omega_{0,1}^{(n)}$ is large by 1·3 per cent

$\omega_{0,2}^{(n)}$ is small by 0·9 per cent

$\omega_{0,3}^{(n)}$ is large by 4·2 per cent

of the average vorticity at the orifice. The large error in $\omega_{0,3}^{(n)}$ is of little consequence since the vorticity on the wall only moves into the half-plane, $x > 0$, by viscous diffusion.

(*c*) *Errors due to nelecting vorticity outside the area covered by the mesh.*—The results for Reynolds number 100 showed that the maximum vorticity on the line $j = 5$ is at $t = 1{\cdot}00$ and $k = 19$. The variation of ω along $k = 19$, 19.05, 22.28, 28.70, 22.07, 10.51, for $j = 1$ to 5, shows that the vorticity at the point (19, 6) would probably be about 5·00. The effect of this vorticity on the velocity at the point (19, 5) would be approximately

$$u_{19,5}^{(n)} = \frac{5\Delta x^2}{2\pi\,\Delta x} \qquad \text{where } \Delta x = 0{\cdot}35 \text{ (curved mesh)}$$

which is 2 per cent of U. The stagnation points in the front whirls would consequently be further from the axis of symmetry than in the results given.

The neglecting of the vorticity outside the mesh would also modify the vorticity at the points $j = 4$ and $j = 5$ at each step in the integration. The error would be greater at $j = 5$ where the approximation to the velocity term, $-\Delta t\{\partial(v\omega)/\partial y\}$ would be too small if $v\omega$ is positive and too large if $v\omega$ is negative. The diffusion term, $\nu\,\Delta t(\partial^2\omega/\partial y^2)$, would also be decreased by a multiple of the vorticity neglected at $j = 6$. At points $j = 5$ behind the front whirls the vorticity will therefore be too small.

(*d*) *Round-off errors.*—It might be expected that the use of numbers of the equivalent of 6 decimal digits would give large round-off errors in the velocity since a large number of terms are added. That this is not so is shown in the results by:

(i) *The symmetry.*—For a symmetrical jet, $\omega_{k,j}^{(n)}$ and $\omega_{k,-j}^{(n)}$, only differed occasionally by unity in the fourth significant decimal digit. In the calculation of the velocity at points (k,j) and $(k, -j)$, the terms involving the vorticity are in pairs of equal magnitude but the round-off errors in the factors $A_{a,b}$ and $A_{a,-b}$, etc., are different (*see* section 3.3). However, the corresponding round-off errors will in general be of the same order.

(ii) The vorticity for a particular point lies on a smooth curve when plotted against time, and at a particular time the graph of vorticity against k is also a smooth curve.

(i) and (ii) are not consistent with the random round-off errors accumulating to a significance level.

In the calculation of the velocity at the point (k,j) the error due to the round-off error in the vorticity at the point (l,m) is only of consequence if the vorticity is multiplied by a large factor which is only so if the points (k,j) and (l,m) are close together. Similarly the round-off errors in the multiplying factor (such as $A_{a,b}$) only gives a large error in the velocity if the vorticity at the point (l,m) is large. Hence for $m_0 = 30$, when there are 1320 terms involving the vorticity in equations (11), the error in the velocity due to round-off errors in $A_{a,b}$, etc., is only important for about $\frac{1}{4}$ of these 1320 terms (since the vorticity is large only along the lines $j = \pm 1, j = \pm 2$).

4.5. *Choice of Time Interval.*—The time interval used throughout was $\Delta t = 0{\cdot}01$. A small time interval has the disadvantage of making the calculation longer to reach a given t (length of calculation $\propto 1/\Delta t$), but to compensate this one may expect increased stability and therefore greater accuracy (provided the Reynolds number is sufficiently high for instability effects to appear). On the other hand, a large time interval, although shortening the calculation, may be expected to show increased instability (section 4.2).

For Reynolds number 100, various time intervals were tried and it was found that increasing the time interval beyond $0{\cdot}01$ gave larger instability oscillations. However, reducing the time interval below $0{\cdot}01$ had little effect on the results. The vorticity for the starting of a symmetrical jet at Reynolds number 100 using the smaller time interval, $\Delta t = 0{\cdot}005$, the velocity being calculated every step (*cf.* section 3.3) was computed and compared with the vorticity for the same calculation using $\Delta t = 0{\cdot}01$. The agreement in the first few steps was remarkable, the greatest difference being unity in the fourth significant digit for $t \leqslant 0{\cdot}05$. Even at $t = 0{\cdot}30$ (which was as far as the calculation was carried) the maximum difference was $0{\cdot}84$ which is less than 2 per cent of the average vorticity at the orifice.

This agreement of results dispels any suspicion that the vortex sheet created at the boundary by taking $v = 0$ might diffuse away in a time interval (In the method of satisfying the condition $v = 0$ at the boundary, the additional vorticity generated during a time interval is introduced at the end of that time interval, thereby excluding the possibility of any significant diffusion or convection of this vorticity during the time interval). Perhaps the explanation lies in the fact that what is referred to as ' additional vorticity generated at the boundary by the condition $v = 0$ ' is not entirely composed of vorticity which has appeared in the last time interval. As an extreme, consider the steady flow when there is a constant velocity near a particular point on the boundary. A constant value of the additional vorticity is generated at that point, the same at the beginning and end of a time interval, so that the method gives the correct diffusion and convection away from the boundary. This boundary vorticity is ' additional ' in the sense that it is added to the vorticity already present in the fluid coming down the entry channel (Equation (12)).

4.6. *Conservation of Vorticity.*—Apart from the fact that random errors arising from different sources may be expected to cancel out to some extent, the difference equations used also have the property that the total vorticity inside an area, S, is independent of time (except for the vorticity transmitted across the boundary of S). Hence, if at a point (k,j) the vorticity at time, $n\,\Delta t$, has an error E introduced in the next step, an error, $-E$, will also be introduced at a neighbouring point, $(k \pm 1,j)$ or $(k,j \pm 1)$, (or spread over several of these neighbouring points).

That this is so may be seen by integrating the terms of equation (3) over the area S.

$$\frac{\partial}{\partial t}\int_S\int \omega\, dx\, dy = \int_S\int \left\{ -\frac{\partial(u\omega)}{\partial x} - \frac{\partial(v\omega)}{\partial y} + \nu\,\frac{\partial^2\omega}{\partial x^2} + \nu\,\frac{\partial^2\omega}{\partial y^2}\right\} dx\, dy$$

$$= \int_C \left\{ -u\omega\, dy + v\omega\, dx + \nu\,\frac{\partial x}{\partial x}\, dy - \nu\,\frac{\partial w}{\partial y}\, dx\right\}$$

where C is the boundary of S,

= the rate at which vorticity flows across the boundary of S.

Similarly, by adding equation (7) for points inside S:

$$\frac{1}{\Delta t}\left\{\sum_S\sum \bar{\omega}_{k,j}^{(n+1)}\,\Delta x^2 - \sum_S\sum \bar{\omega}_{k,j}^{(n)}\,\Delta x^2\right\}$$

$$= \sum_1 \mp \tfrac{1}{2}\left\{\bar{u}_{k,j}^{(n)}\,\bar{\omega}_{k,j}^{(n)}\,\Delta x + \bar{u}_{k\pm1,j}^{(n)}\,\bar{\omega}_{k\pm1,j}^{(n)}\,\Delta x\right\}$$

$$+ \sum_2 \mp \tfrac{1}{2}\left\{\bar{v}_{k,j}^{(n)}\,\bar{\omega}_{k,j}^{(n)}\,\Delta x + \bar{v}_{k,j\pm1}^{(n)}\,\bar{\omega}_{k,j\pm1}^{(n)}\,\Delta x\right\}$$

$$+ \nu\sum_1\left(\bar{\omega}_{k\pm1,j}^{(n)} - \bar{\omega}_{k,j}^{(n)}\right) + \nu\sum_2\left(\bar{\omega}_{k,j\pm1}^{(n)} - \bar{\omega}_{k,j}^{(n)}\right),$$

where the sums on the right-hand side of the equation are over points (k,j) inside K such that:

$$(k \pm 1, j) \text{ lies outside } S \text{ for } \sum_1,$$

$$(k, j \mp 1) \text{ lies outside } S \text{ for } \sum_2.$$

Therefore, omitting the transfer of vorticity across the boundary of S,

$$\sum_S\sum \bar{\omega}_{k,j}^{(n+1)} \Delta x^2 = \sum_S\sum \bar{\omega}_{k,j}^{(n)} \Delta x^2.$$

4.7. *Computer Faults.*—Present day electronic computers are not entirely reliable. Troublesome errors occur due to interference with other nearby electrical equipment, and due to the spasmodic failure of perhaps one element of the vast electronic circuit. These errors occur at random and at intervals of time ranging from a few seconds to several hours.

When an independent check is not possible it is usual to repeat a calculation until two agreeing results are obtained. Because of the random nature of these errors, this result is assumed to be correct.

Because of the abnormal length of these calculations (section 3.2) it was desirable not to do the complete calculations twice. Since an error in the calculation at $t = t_1$ would cause all the results to be wrong for $t > t_1$, it was also desirable to be able to detect an error quickly, and the relevant portion of the calculation repeated. To facilitate repetition of part only of the calculation, at the end of each step a copy of the variables, ω and u, v, was taken out of the computer on punched paper tape in a form that could later be written back into the computer.

The vorticity was also printed out at the end of each step in decimal form and errors were detected as follows:

(*a*) *Symmetry.*—Since, for a symmetrical jet, $\omega_{k,j}^{(n)}$ and $\omega_{k,-j}^{(n)}$ were calculated independently, if $\omega_{k,j}^{(n)} \neq -\omega_{k,-j}^{(n)}$, for any point, a computer fault had occurred.

(*b*) *The graph of ω against t.*—This was a smooth curve. A sudden ' jump ' indicated an error (For this, the graph of a single point on the boundary was sufficient since the vorticity on the boundary depends on the entire vorticity distribution).

(*c*) *The velocity error, E,* (section 3.3).—The majority of calculation was in the evaluation of the velocity so that most computer errors also occurred here. E was a measure of the change of the velocity during a time interval and the maximum change in the velocities already calculated in that step was visible to the operator. The approximate value of E was known (*e.g.*, the value for the previous step) so that an abnormally large change in a velocity caused by a computer fault was thus noticeable. Moreover, this gave a convenient method of checking a velocity whose correctness was suspected. On repeating the calculation of this velocity, obtaining the same values would be indicated by $E = 0$.

In the case of perturbed jets, method (*a*) of detecting computer faults was not available. When the harmonic analysis of the perturbations (section 5.2) was performed, two small errors were detected. This required several nights spent in repeating these solutions.

5. *Perturbations.*—5.1. *Method of Introducing Unsymmetry.*—It was found that with the initial and boundary conditions described above the jet remained symmetrical about the x axis (At $t = 1{\cdot}20$ the maximum of $|\frac{1}{2}\omega_{k,j}^{(n)} + \frac{1}{2}\omega_{k,-j}^{(n)}|$ was $0{\cdot}005$ which is $0{\cdot}01$ per cent of the average vorticity at the orifice). In order to introduce unsymmetry, the boundary condition, $v(0,y,t) = 0$, was modified to:

$$v(o,y,t) = -\varepsilon UF(t) \text{ if } \tfrac{1}{8} \leqslant |y| \leqslant \tfrac{3}{8}$$

$$0 \text{ otherwise}$$

where

$$F(t) = 0 \text{ if } 0 \leqslant t \leqslant 0{\cdot}25$$

$$\sin 2\pi f_1 (t - 0{\cdot}25) + \sin 2\pi f_2 (t - 0{\cdot}25) + \sin 2\pi f_3 (t - 0{\cdot}25)$$

$$\text{if } 0{\cdot}25 \leqslant t.$$

Hence the vorticity at the boundary is given by equation (12):

$$\omega_{0,j}^{(n)} = \bar{\omega}_0(j\,\Delta x,\, n\,\Delta t) + \frac{v_{0,j}^{(n)}}{\Delta y}$$

when $j \neq \pm 1$, and

$$\omega_{0,\pm 1}^{(n)} = \bar{\omega}_0(\pm\Delta x,\, n\,\Delta t) + \frac{1}{\Delta y}\left\{v_{0,\pm 1}^{(n)} + \varepsilon U F(n\,\Delta t)\right\}.$$

The value of ε was taken to be $0{\cdot}00236$ so that $\varepsilon U/\Delta x = 0{\cdot}156$, which is $0{\cdot}3$ per cent of the average vorticity at the orifice.

The values of the frequencies, f_1, f_2, f_3, which could be chosen are bounded above by the use of a finite time interval, $\Delta t = 0{\cdot}01$. Frequencies $100\alpha \pm f$, where α is an integer, would all be indistinguishable so that frequencies greater than 50 are not possible. Hartree (Ref. 14), suggests having at least 6 points per period, which would imply a maximum frequency of 16.

The frequencies were also bounded below since the period of the oscillations, $T = 1/f$, must not be so large that the amount of calculation necessary to complete a period is prohibitive.

The three frequencies used were 5, 10, 15, which have periods $0{\cdot}20$, $0{\cdot}10$, $0{\cdot}07$, units of time. Since the oscillations were commenced at $t = 0{\cdot}25$ ($F(t) = 0$, $0 \leqslant t \leqslant 0{\cdot}25$) and the calculations were carried out up to $t = 0{\cdot}60$, the number of periods completed were $1\frac{3}{4}$, $3\frac{1}{2}$, $5\frac{1}{4}$.

In the tables of results, it is convenient to separate the ' symmetrical ' and ' unsymmetrical ' parts of the vorticity by putting $\omega = \omega_s + \omega_u$ where:

$$(\omega_s)_{k,j}^{(n)} = \tfrac{1}{2}\omega_{k,j}^{(n)} - \tfrac{1}{2}\omega_{k,-j}^{(n)}$$

$$(\omega_u)_{k,j}^{(n)} = \tfrac{1}{2}\omega_{k,j}^{(n)} + \tfrac{1}{2}\omega_{k,-j}^{(n)}.$$

Since the perturbation is small (the three frequencies of oscillation combining to give a maximum of 1 per cent when in phase), the individual frequencies of oscillation are independent. Also ω_s is the vorticity for a symmetrical jet in the absence of the perturbation. For Reynolds number 100, the symmetrical jet was also calculated and the results agree to the 4 decimal places given up to $t = 0{\cdot}36$. Beyond this the velocity was calculated every second step (for the symmetrical jet) so that differences then occur because of this.

5.2. *Harmonic Analysis of* ω_u.—For the frequencies used (f, $2f$ and $3f$ where $f = 5$), $F(t)$ is a periodic function of t of period $0{\cdot}20$ (section 5.1). To the values of $(\omega_u)_{k,j}^{(n)}$ $41 \leqslant n \leqslant 60$, were fitted expressions:

$$\phi(t) = \tfrac{1}{2}A_0 + \sum_{q=1}^{3} A_q \cos 2\pi q f(t - 0{\cdot}25) + B_q \sin 2\pi q f(t - 0{\cdot}25), \quad \ldots \quad (43)$$

where the constants, A_q, B_q, were chosen so that:

$$\sum_{n=41}^{60} \left|\phi(n\,\Delta t) - (\omega_u)_{k,j}^{(n)}\right|^2$$

is a minimum. The values of A_q, B_q are given by:

$$A_q = \frac{1}{10} \sum_{n=41}^{60} (\omega_u)_{k,j}^{(n)} \cos \frac{2\pi qf}{100} (n - 25)$$

$$B_q = \frac{1}{10} \sum_{n=41}^{60} (\omega_u)_{k,j}^{(n)} \sin \frac{2\pi qf}{100} (n - 25).$$

Let

$$\left.\begin{aligned} \tfrac{1}{2}A_0 &= C_0 \\ A_q &= -C_q \sin 2\pi fq\varepsilon_q \quad 1 \leqslant q \leqslant 3 \\ B_q &= +C_q \cos 2\pi fq\varepsilon_q \quad 1 \leqslant q \leqslant 3 \end{aligned}\right\} . \qquad (44)$$

Then

$$\phi(t) = C_0 + \sum_{q=1}^{3} C_q \sin 2\pi qf(t - 0{\cdot}25 - \varepsilon_q).$$

6. *Curved Mesh.*—6.1. *Advantage Over Rectangular Mesh.*—Regions of the half-plane where $\omega = 0$ at time, t, need not be taken into account either in the integration equations, (13) and (14), or in the calculation of velocities (*see* section 3.1). Because of viscous diffusion the region of non-zero vorticity may be expected to extend further in the y direction as x increases. If the calculation were done on a desk machine, allowance would be made for this by changing the size of the rectangular mesh whenever necessary.

It was proposed to do the calculation with the aid of the Manchester University Mark I Computer. In order to simplify the programme of instructions, it was decided to use instead a curved mesh consisting of confocal ellipses and hyperbolae with common foci on the y axis.

6.2. *Vorticity Equation in Curvilinear Co-ordinates.*—The rectangular co-ordinates x, y were replaced by co-ordinates ξ, η such that $x = c \sinh \xi \cos \eta$, $y = c \cosh \xi \sin \eta$, where $c =$ constant.

Let $$h^2 = \frac{\partial(x,y)}{\partial(\xi,\eta)} = c^2(\cosh^2 \xi - \sin^2 \eta).$$

Then $$\frac{\partial^2\omega}{\partial x^2} + \frac{\partial^2\omega}{\partial y^2} = \frac{1}{h^2}\left(\frac{\partial^2\omega}{\partial \xi^2} + \frac{\partial^2\omega}{\partial \eta^2}\right) .$$

Since the fluid is incompressible, there exists a stream function, ψ, such that $u = -\partial\psi/\partial y$, $v = +\partial\psi/\partial x$.

Therefore, the ξ component of velocity, $$U = -\frac{1}{h}\frac{\partial\psi}{\partial\eta}$$

and the η-component of velocity, $$V = +\frac{1}{h}\frac{\partial\psi}{\partial\xi}.$$

$$\begin{aligned} u\frac{\partial\omega}{\partial x} + v\frac{\partial\omega}{\partial y} &= \frac{\partial(\psi,\omega)}{\partial(x,y)} \\ &= \frac{1}{h^2}\frac{\partial(\psi,\omega)}{\partial(\xi,\eta)} \\ &= \frac{1}{h^2}\left(hU\frac{\partial\omega}{\partial\xi} + hV\frac{\partial\omega}{\partial\eta}\right). \end{aligned}$$

Also
$$\frac{\partial(hU)}{\partial\xi} + \frac{\partial(hV)}{\partial\eta} = \frac{\partial}{\partial\xi}\left(-\frac{\partial\psi}{\partial\eta}\right) + \frac{\partial}{\partial\eta}\left(\frac{\partial\psi}{\partial\xi}\right) = 0.$$

Therefore equation (3) becomes:

$$\frac{\partial\omega}{\partial t} + \frac{1}{h^2}\left\{\frac{\partial(hU\omega)}{\partial\xi} + \frac{\partial(hV\omega)}{\partial\eta}\right\} = \frac{\nu}{h^2}\left\{\frac{\partial^2\omega}{\partial\xi^2} + \frac{\partial^2\omega}{\partial\eta^2}\right\}. \quad .. \quad .. \quad (3)'$$

6.3. *Velocity Coefficients.*—Consider a set of mesh points (k,j) given by $x = c \sinh k\Delta \cos j\Delta$, $y = c \cosh k\Delta \sin j\Delta$, in which $\Delta\xi = \Delta\eta = \Delta =$ constant and where k and j are integers. Let Q be the point (k,j), P be the point (m,l), $PQ = r$, $\theta =$ angle between PQ and the x axis; and $\phi =$ angle at Q between the curve $\eta =$ constant and the x axis (*see* Fig. 8).

Consider the velocity at Q due to a point vortex at P of strength ω. Let $U^{(n)}_{k,j}$, $V^{(n)}_{k,j}$ be the components of velocity at Q parallel to the curves $\eta =$ constant, $\xi =$ constant. Let $h_{k,j} = c\,(\cosh^2 k\Delta - \sin^2 j\Delta)^{1/2}$ $(h_{k,j} \geqslant 0)$

$$a = k - m,$$

$$a' = k + m,$$

$$b = j - l,$$

$$b' = j + l.$$

Then
$$U^{(n)}_{k,j} = -\frac{\omega}{2\pi r}\sin(\theta - \phi),$$

$$V^{(n)}_{k,j} = \frac{\omega}{2\pi r}\cos(\theta - \phi),$$

where
$$\sin\theta = \frac{c}{r}(\cosh k\Delta \sin j\Delta - \cosh m\Delta \sin l\Delta),$$

$$\cos\theta = \frac{c}{r}(\sinh k\Delta \cos j\Delta - \sinh m\Delta \cos l\Delta),$$

$$\sin\phi = \frac{c}{h_{k,j}}\sinh k\Delta \sin j\Delta,$$

$$\cos\phi = \frac{c}{h_{k,j}}\cosh k\Delta \cos j\Delta.$$

Now,
$$\frac{r^2}{c^2} = (\cosh k\Delta \sin j\Delta - \cosh m\Delta \sin l\Delta)^2$$

$$+ (\sinh k\Delta \cos j\Delta - \sinh m\Delta \cos l\Delta)^2$$

$$= (\cosh a\Delta - \cos b\Delta)(\cosh a'\Delta + \cos b'\Delta).$$

Therefore:

$$h_{k,j}\,U^{(n)}_{k,j} = \frac{\omega c^2}{2\pi r^2}\{-(\cosh k\Delta \sin j\Delta - \cosh m\Delta \sin l\Delta)\cosh k\Delta \cos j\Delta$$

$$+ (\sinh k\Delta \cos j\Delta - \sinh m\Delta \cos l\Delta)\sinh k\Delta \sin j\Delta\}$$

$$= \frac{\omega}{4\pi}\left\{\frac{\sin b'\Delta}{\cos a'\Delta + \cos b'\Delta} - \frac{\sin b\Delta}{\cos a\Delta - \cos b\Delta}\right\},$$

and similarly

$$h_{k,j}\,V^{(n)}_{k,j} = \frac{\omega}{4\pi}\left\{\frac{\sinh a'\Delta}{\cosh a'\Delta + \cos b'\Delta} + \frac{\sinh a\Delta}{\cosh a\Delta - \cos b\Delta}\right\}.$$

Similarly the velocity at the point Q due to the image vortex of strength $\omega' = -\omega$ at the point P' $(-m,l)$ is given by:

$$h_{k,j}\,U^{(n)}_{k,j} = \frac{\omega'}{4\pi}\left\{\frac{\sin b'\Delta}{\cosh a\Delta + \cos b'\Delta} - \frac{\sin b\Delta}{\cosh a'\Delta - \cos b\Delta}\right\},$$

$$h_{k,j}\,V^{(n)}_{k,j} = \frac{\omega'}{4\pi}\left\{\frac{\sinh a\Delta}{\cosh a\Delta + \cos b'\Delta} + \frac{\sinh a'\Delta}{\cosh a'\Delta - \cos b\Delta}\right\}.$$

Therefore the velocity at Q due to both the vortex ω at P and the image vortex ω' at P' is given by:

$$h_{k,j}\,U^{(n)}_{k,j} = \frac{\omega}{4\pi}\left\{-\frac{\sin b\Delta}{\cosh a\Delta - \cos b\Delta} - \frac{\sin b'\Delta}{\cosh a\Delta + \cos b'\Delta}\right\}$$

$$+ \frac{\omega'}{4\pi}\left\{-\frac{\sin b\Delta}{\cosh a'\Delta - \cos b\Delta} - \frac{\sin b'\Delta}{\cosh a'\Delta + \cos b'\Delta}\right\}$$

$$h_{k,j}\,V^{(n)}_{k,j} = \frac{\omega}{4\pi}\left\{\frac{\sinh a\Delta}{\cosh a\Delta - \cos b\Delta} - \frac{\sinh a\Delta}{\cosh a\Delta + \cos b'\Delta}\right\}$$

$$+ \frac{\omega'}{4\pi}\left\{\frac{\sinh a'\Delta}{\cosh a'\Delta - \cos b\Delta} - \frac{\sinh a'\Delta}{\cosh a'\Delta + \cos b'\Delta}\right\}.$$

Now for a continuous distribution of vorticity, the vorticity in the region, $m\Delta - \frac{1}{2}\Delta \leqslant \xi \leqslant m\Delta + \frac{1}{2}\Delta$, $l\Delta - \frac{1}{2}\Delta \leqslant \eta \leqslant l\Delta + \frac{1}{2}\Delta$, is replaced by a point vortex of strength, $\omega^{(n)}_{m,l}\,h^2_{m,l}\,\Delta^2$, at the point (m,l).

Let

$$A_{a,b} = -\frac{\Delta}{4\pi}\frac{\sin b\Delta}{\cosh a\Delta - \cos b\Delta}, \text{ if } a \neq 0 \text{ or } b \neq 0$$

$$B_{a,b} = +\frac{\Delta}{4\pi}\frac{\sin b\Delta}{\cosh a\Delta + \cos b\Delta}$$

$$D_{a,b} = +\frac{\Delta}{4\pi}\frac{\sinh a\Delta}{\cosh a\Delta - \cos b\Delta}, \text{ if } a \neq 0 \text{ or } b \neq 0,$$

$$E_{a,b} = +\frac{\Delta}{4\pi}\frac{\sinh a\Delta}{\cosh a\Delta + \cos b\Delta}$$

and

$$A_{0,0} = D_{0,0} = 0.$$

Therefore the velocity at Q due to the source flow is given by:

$$\left.\begin{aligned} \frac{h_{k,j}U^{(n)}_{k,j}}{\Delta} &= \sum_{l=-l_1}^{l_1} C_{k,j,l}\,\bar{u}_0(l\,\Delta y,\, n\,\Delta t) \\ \frac{h_{k,j}V^{(n)}_{k,j}}{\Delta} &= \sum_{l=-l_1}^{l_1} F_{k,j,l}\,\bar{u}_0(l\,\Delta y,\, n\,\Delta t) \end{aligned}\right\} \quad \ldots \quad (10)'$$

Hence the resultant velocity at Q due to both the vorticity and source flow is given by:

$$\left.\begin{aligned} \frac{h_{k,j}U^{(n)}_{k,j}}{\Delta} &= \left(\sum_{m=-m_0}^{-1} + \sum_{m=1}^{m_0}\right) \sum_{l=-l_0}^{l_0} (A_{k-m,j-l} - B_{k-m,j+l}) h^2_{m,l}\,\omega^{(n)}_{m,l} \\ &\quad + \sum_{l=-l_1}^{l_1} C_{k,j,l}\,\bar{u}_0(l\,\Delta y,\, n\,\Delta t) \\ \frac{h_{k,j}V^{(n)}_{k,j}}{\Delta} &= \left(\sum_{m=-m_0}^{-1} + \sum_{m=1}^{m_0}\right) \sum_{l=-l_0}^{l_0} (D_{k-m,j-} - E_{k-m,j+l}) h^2_{m,l}\,\omega^{(n)}_{m,l} \\ &\quad + \sum_{l=-l_1}^{l_1} F_{k,j,l}\,\bar{u}_0(l\,\Delta y,\, n\,\Delta t) \end{aligned}\right\} \quad \ldots \quad (11)'$$

6.4. *Finite-Difference Equations.*—When the finite difference approximations corresponding to (6) are substituted in equation (3)′, one obtains:

$$\omega^{(n+1)}_{k,j} = \omega^{(n)}_{k,j} + F(U^{(n)}_{K,J},\, V^{(n)}_{K,J},\, \omega^{(n)}_{K,J}) \quad \ldots \quad (7)'$$

in which K takes the values $k \pm 1, k$,

J takes the values $j \pm 1, j$,

and where

$$\begin{aligned} F(U^{(n)}_{K,J},\, V^{(n)}_{K,J},\, \omega^{(n)}_{K,J}) = \frac{\Delta t}{2h^2_{k,j}} \Bigg\{ & \frac{h_{k-1,j}\,U^{(n)}_{k-1,j}}{\Delta}\,\omega^{(n)}_{k-1,j} - \frac{h_{k+1,j}\,U^{(n)}_{k+1,j}}{\Delta}\,\omega^{(n)}_{k+1,j} \\ & + \frac{h_{k,j-1}\,V^{(n)}_{k,j-1}}{\Delta}\,\omega_{k,j-1} - \frac{h_{k,j+1}\,V^{(n)}_{k,j+1}}{\Delta}\,\omega^{(n)}_{k,j+1} \Bigg\} \\ & + \frac{\nu\,\Delta t}{h^2_{k,j}\,\Delta^2} \left\{ \omega^{(n)}_{k+1,j} + \omega^{(n)}_{k-1,j} + \omega^{(n)}_{k,j+1} + \omega^{(n)}_{k,j-1} - 4\omega^{(n)}_{k,j} \right\}. \end{aligned}$$

Also, from equation (12), the vorticity at points on the boundary is given by:

$$\omega^{(n)}_{0,j} = \bar{\omega}_0(c \sin j\Delta,\, n\,\Delta t) + \frac{1}{h^2_{0,j}} \frac{h_{0,j}\,V^{(n)}_{0,j}}{\Delta} \quad \ldots \quad (12)'$$

6.5. *Arrangement of Stores.*—The constant coefficients, $A_{a,b}$, $B_{a,b}$, $C_{k,j,l}$, $D_{a,b}$, $E_{a,b}$, $F_{k,j,l}$, $h^2_{k,j}$, $1/h^2_{k,j}$, which were used repeatedly were first calculated and kept permanently in the slow-speed magnetic store. They were also obtained on punched paper tape and could be quickly ' written ' into the store at the beginning of a run.

For each value of a, $4l_0 + 1$ values of each of $A_{a,b}$, $B_{a,b}$, $D_{a,b}$, $E_{a,b}$, were required (Only $2l_0 + 1$ of these are independent because of the symmetry relations.

$$A_{a,-b} = -A_{a,b},$$

$$B_{a,-b} = -B_{a,b},$$

$$D_{a,-b} = +D_{a,b},$$

$$E_{a,-b} = +E_{a,b}).$$

For each value of k, $(2l_0 + 1)(l_1 + 1)$ independent values of $C_{k,j,l}$ and $F_{k,j,l}$ were required (We have

$$C_{k,-j,l} = +C_{k,j,l},$$

$$F_{k,-j,l} = +F_{k,j,l}).$$

Short lines, consisting of 20 binary digits (which is approximately equivalent to 6 decimal digits) were used throughout. Since the magnetic store is divided into tracks (These sections of the store are such that transfers to and from the magnetic store can be carried out in complete tracks or in complete half-tracks) consisting of 128 short lines, the values $l_0 = 5$, $l_1 = 4$, were chosen. This enabled $A_{a,b}$, $B_{a,b}$, $D_{a,b}$, $E_{a,b}$, for all necessary values of b to be stored on one half-track for each value of a. Also $C_{k,j,l}$, $F_{k,j,l}$, for all necessary j and l were stored on one full track for each value of k.

At each step in the integration it was also desired to keep the variables,

$$\omega_{k,j}^{(n)},\ \Omega_{k,j}^{(n+1)},$$

$$\frac{h_{k,j}\,U_{k,j}^{(n)}}{\Delta},\ \frac{h_{k,j}\,V_{k,j}^{(n)}}{\Delta},$$

in the magnetic store.

For each value of k there were 11 of each of these, which together with the 6 independent values of $h_{k,j}^2$ and 6 independent values of $1/h_{k,j}^2$ (We have $h_{k,-j} = h_{k,j}$) were also stored on one half-track.

7. *Results.*—7.1. *List of Computations Done:*

(*a*) The starting of a symmetrical jet at Reynolds number 100. 120 time steps.

(*b*) The starting of a symmetrical jet at Reynolds numbers 50, 100, 150, 300. 60 time steps.

(*c*) The perturbation at frequencies 5, 10, 15, of a jet at Reynolds numbers 50, 100, 150, 300. 60 time steps.

For each Reynolds number, the calculations (*b*) and (*c*) were done simultaneously, the symmetrical jet being given by ω_s and the perturbation by ω_u (*see* section 5.1).

7.2. *Numerical Values.*—The equation of motion, (3), may be put in non-dimensional form as follows.

Let $x = dx'$ where d = constant = width of orifice

$y = dy'$

$u = Uu'$ where U = constant = average velocity at the orifice

$$v = Uv'$$

$$t = \frac{d}{U}t'.$$

Then $\omega = (U/d)\omega'$ where $\omega' = (\partial v'/\partial x') - (\partial u'/\partial y')$.

Then (3) becomes:

$$\frac{\partial \omega'}{\partial t'} + \frac{\partial (u'\omega')}{\partial x'} + \frac{\partial (v'\omega')}{\partial y'} = \frac{1}{R}\left(\frac{\partial^2 \omega'}{\partial x'^2} + \frac{\partial^2 \omega'}{\partial y'^2}\right),$$

where $R = Ud/\nu$ is the Reynolds number of the flow.

Throughout, the values $d = 1$, $U = 16{\cdot}54$, were taken.

Also $u_0(y,t)$ was given by:

$$u_0(y,t) = Uf(t)\,g(y), \quad .. \quad .. \quad .. \quad .. \quad .. \quad .. \quad .. \quad .. \quad (43)$$

where

$$g(y) = 1{\cdot}5 - 6y^2 \text{ if } |y| \leqslant \tfrac{1}{2},$$

$$0 \qquad \text{if } |y| \geqslant \tfrac{1}{2},$$

and

$$f(t) = 32t^2 \qquad \text{if } 0 \leqslant t \leqslant 0{\cdot}125,$$

$$1 - 32(0{\cdot}25 - t)^2 \text{ if } 0{\cdot}125 \leqslant t \leqslant 0{\cdot}25,$$

$$1 \qquad \text{if } 0{\cdot}25 \leqslant t.$$

The parabolic distribution of velocity, $g(y)$, is what is obtained for a steady laminar viscous flow between two infinite parallel planes.

The maximum velocity is reached in the time taken for the fluid in the entry channel (moving with velocity, $Uf(t)$) to travel a distance $2{\cdot}07$ diameters.

The coefficient of viscosity, ν, $= 0{\cdot}1641$ so that $R = 100{\cdot}8$. This will be referred to as '$R = 100$'. Results were also obtained for '$R = 50$', '$R = 150$', '$R = 300$' which are for $\nu = 2$, $2/3$, and $1/3$ of this value respectively and with the same boundary conditions.

The mesh points were taken as $x = c \sinh k\Delta \cos j\Delta$, $y = c \cosh k\Delta \sin j\Delta$, where k, j are integers and $c = 5{\cdot}319$, $\Delta = 0{\cdot}4707$. Hence the confocal ellipses and hyperbolae, comprising the mesh lines, have their two common foci on the y axis at a distance $5{\cdot}319d$ from the origin.

Also $k = 0$, $j = 2$ gives the point $x = 0$, $y = d/2$ at the edge of the orifice $\Delta y = \frac{1}{4}$.

The values of $\bar{\omega}_0(c \sin j\Delta, t)/f(t)$ in equation (12)′ were taken as $\pm\ 50{\cdot}00$ for $j = \pm\ 1$, $\pm\ 43{\cdot}75$ for $j = \pm\ 2$, $+\ 0{\cdot}00$ otherwise.

The values of $u_0(j\,\Delta y, t)/f(t)$ were $24{\cdot}29$ for $j = 0$, $18{\cdot}09$ for $j = \pm\ 1$, $2{\cdot}84$ for $j = \pm\ 2$, $0{\cdot}00$ otherwise.

$\Delta t = 0{\cdot}01$ was used throughout.

7.3. *Starting of a Symmetrical Jet.*—At first the velocity is approximately radial, being everywhere directed along the line through the centre of the orifice. Since very little vorticity has spread into the half-plane, the velocity is almost entirely given by the source flow. The velocity near the wall is also directed away from the orifice and quite a large value of the vorticity is

generated at the wall. Since this vorticity can only spread into the half-plane by viscous diffusion (as the velocity component perpendicular to the wall is zero), it remains near the wall and consequently has little effect on the flow. Similarly the velocity component parallel to the boundary generates vorticity at the orifice (at the points $(0, \pm 1)$, $(0, \pm 2)$ and for $t \leqslant 0{\cdot}07$ this amounts to approximately half the values given for the vorticity at these points. The magnitude of the contribution to the vorticity at the boundary, given by enforcing the condition $v = 0$, continues to increase with time and, for the points considered (which are near the origin) reaches a maximum about $t = 0{\cdot}15$. The effect on the velocity at the boundary due to the vorticity which is spreading into the half-plane is now increasing at the same rate as the effect of the increasing flow at the entry (Graph 1).

At $t = 0{\cdot}25$, when $u_0(y,t)$ has reached its final steady value, the effects at the boundary of the vorticity in the half-plane and of the source flow are approximately equal and opposite, the velocity along the wall having changed to an inflow towards the orifice at the points $(0, \pm 3)$ and $(0, \pm 4)$ (Graph 2). There is a stagnation point on the wall between the points (0, 4) and (0, 5). This stagnation point will always exist at some point on the wall. The velocity component v at any time at a point $(0, r)$ on the wall a distance r from the origin is given by:

$$\left.\begin{aligned} v &= -\frac{1}{2\pi}\int_0^\infty\int_0^\infty \frac{\omega x\,dx\,dy}{x^2+(r-y)^2} + \frac{1}{2\pi}\int_0^\infty\int_0^\infty \frac{\omega x\,dx\,dy}{x^2+(r+y)^2} \\ &= -\frac{2}{\pi}\int_0^\infty\int_0^\infty \frac{\omega xyr\,dx\,dy}{\{x^2+(r-y)^2\}\{x^2+(r+y)^2\}} \end{aligned}\right\}, \quad \ldots \quad \ldots \quad (45)$$

$$\sim \frac{K}{r^3} \text{ as } r \to \infty,$$

where K = constant, assuming the integral (45) to be uniformly convergent with respect to r.

However, the velocity due to the source flow $\sim M/\pi r$ as $r \to \infty$ where:

$$M = \int_{-\infty}^{\infty} u_0(y,t)\,dy.$$

For sufficiently large r the latter predominates and since M is positive the velocity is directed outwards from the orifice.

At $t = 0{\cdot}25$ the flow first begins to take up the ' mushroom ' form which characterises it from then on (Graphs 2 to 5). The vorticity moves out in a ' front ' consisting of a large amount of vorticity. Beyond the front the radial velocity of the source flow is diverted away from the line of symmetry $y = 0$, and just behind it are produced quite large velocities directed towards the line of symmetry. Within the front there is a stagnation point where the fluid is instantaneously at rest (and which at $t = 0{\cdot}25$ is near the stagnation point on the wall).

Hence the front consists of two large ' whirls ', one on either side of the axis of symmetry, similar to a vortex pair in a perfect fluid. The fluid particles which make up these front whirls are continually changing since the streamlines are not particle paths.

The front whirls leave behind them an almost steady flow. From $t = 1{\cdot}00$ to $t = 1{\cdot}20$ the velocity and vorticity at no point changed by more than 5 per cent of the average values at the orifice for $x \leqslant 3$ diameters, and from $t = 1{\cdot}19$ to $t = 1{\cdot}20$ the vorticity in this region changed by less than $0{\cdot}1$ per cent. This steady flow consists in the jet continuing from the orifice unchanged except that as x increases more of the neighbouring fluid is accelerated from rest to move with the jet, which increases in velocity as it widens. The high velocity gradient present in the jet at the orifice diffuses away as the fluid moves downstream (*cf.* Bickley's jet shown in Graph 6).

The simplification of omitting the velocity calculation was first introduced in the 37th step, the velocity being calculated only in the even numbered steps for $36 \leqslant n \leqslant 84$, and only if n was divisible by 4 for $84 \leqslant n \leqslant 120$. The maximum error introduced in the vorticity by omitting the velocity calculation in s consecutive steps (less than 4 per cent (section 3.3)) occurred in the front whirls and this error decreased, though not always monotonically, as one passed to points nearer the boundary. If the error in the points $k = k_1$, $-5 \leqslant j \leqslant 5$, that would have been introduced through only calculating the velocity every $2s$th step became less than $1 \cdot 5$ per cent no further velocities ($k < k_1$) were calculated in that step. Usually this meant that the velocity was not calculated at 1/3 of those points where the velocity was required. The error introduced in doing this was probably less than $1 \cdot 5$ per cent and certainly less than 4 per cent. However, every second time the velocity was calculated it was calculated at every point of the mesh behind the front whirls.

7.4. *Effect of Reynolds Number.*—Results were also obtained for a symmetrical jet at Reynolds numbers 50, 100, 150, 300. These calculations were actually performed with a small unsymmetrical perturbation superimposed, the symmetrical flow being given by:

$$(\omega^{(n)}_{k,j})_{\text{symmetrical}} = \tfrac{1}{2}\omega^{(n)}_{k,j} - \tfrac{1}{2}\omega^{(n)}_{k,-j}.$$

In these calculations the velocity was computed in every step.

For Reynolds number 100, the results obtained in this way agree to 4 significant decimal digits with the results obtained previously up to $t = 0 \cdot 36$. From then on differences appear, since in the first calculation the velocity was then only computed every second step. For $t = 0 \cdot 60$ this difference is greatest at the points $(11, \pm 4)$ being there 8 per cent of the average vorticity at the orifice.

These flows were also started from rest and with the same boundary conditions, (4) and (5), the different Reynolds numbers being obtained by using different values for the coefficient of viscosity, ν. Calculations were carried up to $t = 0 \cdot 60$.

The velocity and vorticity distributions show little variation with Reynolds number in the time when the velocity at the orifice is increasing ($t \leqslant 0 \cdot 25$). After $t = 0 \cdot 25$ the jet widens more for lower Reynolds numbers, the velocity in the jet becoming correspondingly smaller. At $t = 0 \cdot 60$ the velocity for Reynolds number 50 is much smaller than for the higher Reynolds numbers, and the large values of the vorticity at the orifice rapidly decrease as the fluid moves downstream (Graph 7). The front whirls at $t = 0 \cdot 60$ also shown considerable variation with Reynolds number. For a lower Reynolds number, the front whirls:

(*a*) do not travel so far downstream
(*b*) rotate less rapidly
(*c*) have the smaller vorticity comprising them spread over a larger area. The velocity of the inflow near the wall decreases as the Reynolds number increases.

Except for Reynolds number 50, the vorticity distributions show periodic variation with k along the lines $j = \pm 1$ (Graphs 13 and 14). The amplitude of these oscillations increases with Reynolds number and for $R = 300$ also increases with time. This is attributed to the instability of the finite-difference equations (section 4.1). For $R = 300$ it cannot be a feature of the actual flow (which is the solution of the differential equation) since a maximum value of the vorticity at a point not on the boundary must decrease with time. (In cartesian co-ordinates:

$$\frac{D\omega}{Dt} = \frac{\partial \omega}{\partial t} + u\frac{\partial \omega}{\partial x} + v\frac{\partial \omega}{\partial y}$$

$$= \nu\left(\frac{\partial^2 \omega}{\partial x^2} + \frac{\partial^2 \omega}{\partial y^2}\right)$$

$$< 0).$$

Although the amplitude of these oscillations in the vorticity distribution is large, the effect on the velocity is small. Oscillations in the velocity are only really noticeable for $R = 300$ when the vorticity variation along the line $j = 1$ is of the same order as the average vorticity at the orifice.

7.5. *Perturbations.*—The perturbations were introduced at $t = 0{\cdot}25$ so that at $t = 0{\cdot}25$, $\omega_u = 0$ everywhere. In the next 5 steps $F(t) > 0$ and positive vorticity is convected along the lines $j = \pm 1$. This positive vorticity increases the velocity component v at points further from the orifice which causes the appearance of negative values of ω_u at points $j = 0, \pm 1$, where the vorticity gradient in the y direction is large and positive. Also, this positive vorticity produces a negative velocity component v near the boundary which generates negative vorticity.

More information is obtained by examining the three Fourier components of the perturbation, ω_u. Separate computations could have been done, each with a single frequency, but since the amplitudes used were small (for the 3 frequencies in phase the value of ω_u at the orifice is 1 per cent of the average vorticity) the method adopted (using harmonic analysis) will give the same results more rapidly.

For Reynolds numbers 50, 100, 150, 300, C_q and ε_q were calculated and C_q are given in Graphs 17 to 19. Along $j = 0, \pm 1, \pm 2$, C_q is seen to increase with Reynolds number. This is partly due to the fact that $(\omega_s)^{(n)}_{k,j}$ increases with Reynolds number. Except for the two higher frequencies at Reynolds number 50, along $j = 0, \pm 2$, C_q also increases with k for $k < 8$ which is behind the front whirls. Since $\omega^{(n)}_{kj} = 0$ for large k, $C_q = 0$ for large k.

At most points, $C_1 > C_2 > C_3$ showing that the lowest frequency oscillation ($f_1 = 5$) is least stable. For Reynolds number 50, the higher frequency oscillations (10 and 15) are quickly damped out as the fluid moves away from the orifice.

The definition of ε_q by equations (44) is not unique since if ε_q satisfies equation (44), so also does:

$$\varepsilon_q' = \varepsilon_q + \frac{\alpha}{5q},$$

where α is any integer. The particular value of ε_q was chosen so that:

$$(a) \quad (\varepsilon_q)_{k,j} + \frac{1}{5q} \geqslant (\varepsilon_q)_{k+1,j} > (\varepsilon_q)_{k,j}$$

$$(b) \quad 0 \geqslant (\varepsilon_q)_{0,j} > -\frac{1}{5q}.$$

From the graph of ε_q it was seen that ε_q was approximately a linear function of x. Let $\varepsilon_q = (1/c)x + d$, where c, d are constants. Then c is the phase velocity of the qth of frequency oscillation. The value of c obtained from the graphs was:

$j = 0$			$j = 1$			R
$q = 1$	$q = 2$	$q = 3$	$q = 1$	$q = 2$	$q = 3$	
12	15	21	11	10	14	50
13	13	15	12	10	17	100
13	13	14	11	11	17	150
				11	11	300

which have averages of 14 and 12. The third frequency of oscillation appears to travel more quickly than the other two, the average value of c for it being 17 for $j = 0$ and 15 for $j = 1$.

The phase velocity is less than the fluid velocity, the latter being 24 for $j = 0$ and 18 for $j = 1$ at the orifice.

REFERENCES

No.	Author	Title, etc.
1	E. N. da C. Andrade	*Proc. Phys. Soc. Lond.* 51. pp. 784 to 793. 1937.
2	W. G. Bickley	*Phil. Mag.* 7. 23. pp. 727 to 731. 1937.
3	F. H. Bushby and M. K. Hinds	*Q. J. Roy. Met. Soc.* 80. No. 344. 1954.
4	R. Courant, K. O. Friedrichs and H. Lewy	*Math. Annalen.* 100. pp. 32 to 64. 1928.
5	J. Crank and P. Nicholson ..	*Proc. Camb. Phil. Soc.* 43. pp. 50 to 67. 1947.
6	N. Curl	*Proc. Roy. Soc.* A.216. pp. 412 to 424. 1953.
7	D. R. Hartree	*Numerical Analysis.* Oxford University Press. 1952.
8	F. John	*Comm. on Pure and App. Maths.* 5. pp. 155 to 211. 1952.
9	Sir H. Lamb	*Hydrodynamics.* Cambridge University Press. 6th Edition.
10	P. D. Lax	*Comm. on Pure and App. Maths.* 7. pp. 159 to 193. 1954.
11	J. Neumann and R. D. von Ritchmyer	*J. App. Phys.* 29. pp. 232 to 237. 1950.
12	G. G. O'Brien, M. A. Hyman and S. Kaplan	*J. Math. Phys.* 29. pp. 223 to 251. 1950.
13	L. F. Richardson	*Phil. Trans. Roy. Soc.* Series A.210. pp. 307 to 357. 1910.
14	P. Savic	*Phil. Mag.* 7. 320. pp. 245 to 252. 1941.

LEGEND

Graphs 1 *to* 5. The starting of a symmetrical jet at Reynolds number 100. Because of the symmetry only one half of each graph is given.

(*a*) Contours of equal vorticity ($\omega = 1, 10, 20, 30, 40, 50$) are shown in the upper half of the graphs. The line of symmetry, OX, is the contour $\omega = 0$.

(*b*) The streamlines are shown in the lower half of the graphs. In drawing these an attempt was made to space the streamlines inversely as the velocity magnitude. The line of symmetry, OX, is one of this system of streamlines.

Graph 1 is for $t = 0{\cdot}15$,

Graph 2 is for $t = 0{\cdot}25$,

Graph 3 is for $t = 0{\cdot}45$,

Graph 4 is for $t = 0{\cdot}80$,

Graph 5 is for $t = 1{\cdot}20$.

Graph 6. The steady flow of a jet at Reynolds number 100 as given by Bickley's solution. Vorticity contours and streamlines are drawn as in Graphs 1 to 5.

Graphs 7 *to* 10. The starting of a symmetrical jet for different Reynolds numbers. Vorticity contours and streamlines at $t = 0{\cdot}60$ are drawn as in Graphs 1 to 6.

Graph 7 is for Reynolds number 50,

Graph 8 is for Reynolds number 100,

Graph 9 is for Reynolds number 150,

Graph 10 is for Reynolds number 300.

Graph 11. Vorticity against time at points on the line $j = 1$ for the starting of a symmetrical jet at Reynolds number 100.

$k = 0$ is $x = 0{\cdot}0$, $y = 0{\cdot}25$ (at the orifice),

$k = 4$ is $x = 1{\cdot}0$, $y = 0{\cdot}25$,

$k = 8$ is $x = 2{\cdot}0$, $y = 0{\cdot}27$,

$k = 12$ is $x = 3{\cdot}2$, $y = 0{\cdot}29$,

$k = 16$ is $x = 4{\cdot}4$, $y = 0{\cdot}32$,

$k = 24$ is $x = 7{\cdot}4$, $y = 0{\cdot}43$.

Graph 12. Vorticity against time at points on the lines $j = 2$ and $j = 4$ for the starting of a symmetrical jet at Reynolds number 100.

$j = 2$,

$k = 0$ is $x = 0{\cdot}0$, $y = 0{\cdot}5$ (at the edge of the orifice),

$k = 4$ is $x = 1{\cdot}0$, $y = 0{\cdot}5$,

$k = 8$ is $x = 2{\cdot}0$, $y = 0{\cdot}5$,

$k = 12$ is $x = 3{\cdot}2$, $y = 0{\cdot}6$,

$k = 16$ is $x = 4{\cdot}4$, $y = 0{\cdot}6$,

$k = 24$ is $x = 7{\cdot}4$, $y = 0{\cdot}9$.

$j = 4$,

$k = 0$ is $x = 0{\cdot}0$, $y = 1{\cdot}0$ (on the wall),

$k = 4$ is $x = 1{\cdot}0$, $y = 1{\cdot}0$,

$k = 8$ is $x = 2{\cdot}0$, $y = 1{\cdot}1$,

$k = 12$ is $x = 3{\cdot}1$, $y = 1{\cdot}2$,

$k = 16$ is $x = 4{\cdot}3$, $y = 1{\cdot}3$,

$k = 24$ is $x = 7{\cdot}2$, $y = 1{\cdot}7$.

Graph 13. Vorticity against time at points on the line $j = 1$ for the starting of a symmetrical jet at Reynolds number 50.

Graph 14. Vorticity against time at points on the line $j = 1$ for the starting of a symmetrical jet at Reynolds number 150. At Reynolds number 300 the vorticity at points on $j = 1$ showed bigger oscillations which increased in amplitude as t increased.

Graph 15. Vorticity against time at points on the lines $j = 2$ and $j = 4$ for the starting of a symmetrical jet at Reynolds number 50.

Graph 16. Vorticity against time at points on the lines $j = 2$ and $j = 4$ for the starting of a symmetrical jet at Reynolds number 150. At Reynolds number 300 the vorticity at points on $j = 2$ was further increased, and at points on $j = 4$ was further reduced.

Graphs 17 *to* 19. The amplitudes, C_1, C_2, C_3, of the unsymmetrical sinusoidal oscillations in the vorticity for the perturbed jet plotted against k.

$$\omega_u = C_0 + \sum_{q=1}^{3} C_q \sin 2\pi q f(t - 0{\cdot}25 - \varepsilon_q),$$

The vorticity, ω_s, for the corresponding symmetrical jet at $t = 0{\cdot}60$, is also given for comparison (*see* Section 5·2). Away from the center-line of the jet (on $j = 3$, 4 and 5) these amplitudes were found to be small.

Graph 17 is for Reynolds number 50,

Graph 18 is for Reynolds number 100,

Graph 19 is for Reynolds number 150.

For Reynolds number 300 the graph of vorticity against k for points on $j = 1$ for the symmetrical jet showed very large oscillations. The perturbation amplitudes were also larger.

Graph 20. Critical stability curves. The time interval ratio, $\Delta t/\Delta x$, for various Reynolds numbers (based on the mesh width, Δx).

$$R_m = \text{The Reynolds number of the mesh} \times 4$$

$$= \frac{u\,\Delta x}{\nu} 4.$$

$$L = \frac{u}{2}\frac{\Delta t}{\Delta x}.$$

For larger time intervals the difference equation is unstable and unbounded (*see* Section 4.2).

(*a*) Forward time-difference (equation (7))

(*b*) Improved time difference (equation (13))

(*c*) $h(X)/X$ which was used to determine graph (b)

(*d*) $R_m = 32L$.

(c) is also a critical stability curve (R_m/L) for the improved time difference equation (equation 13)).

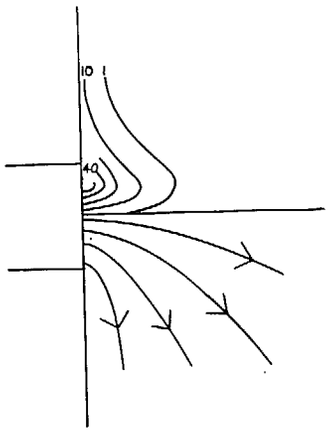

GRAPH 1.

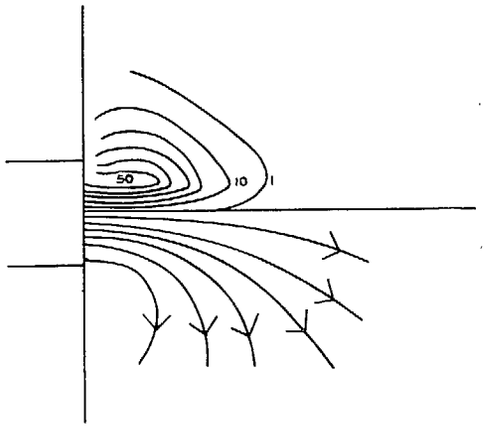

GRAPH 2.

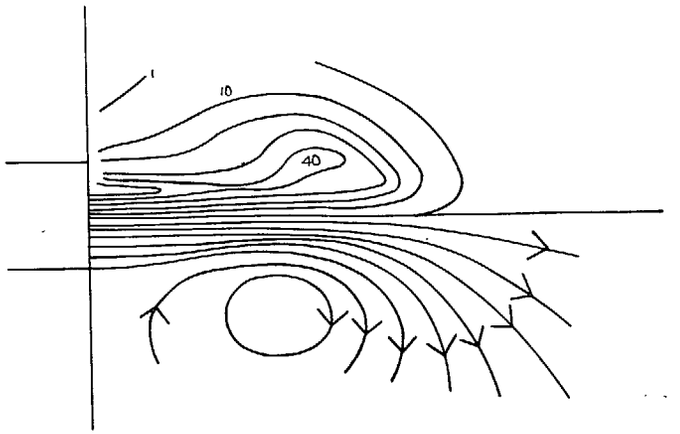

GRAPH 3.

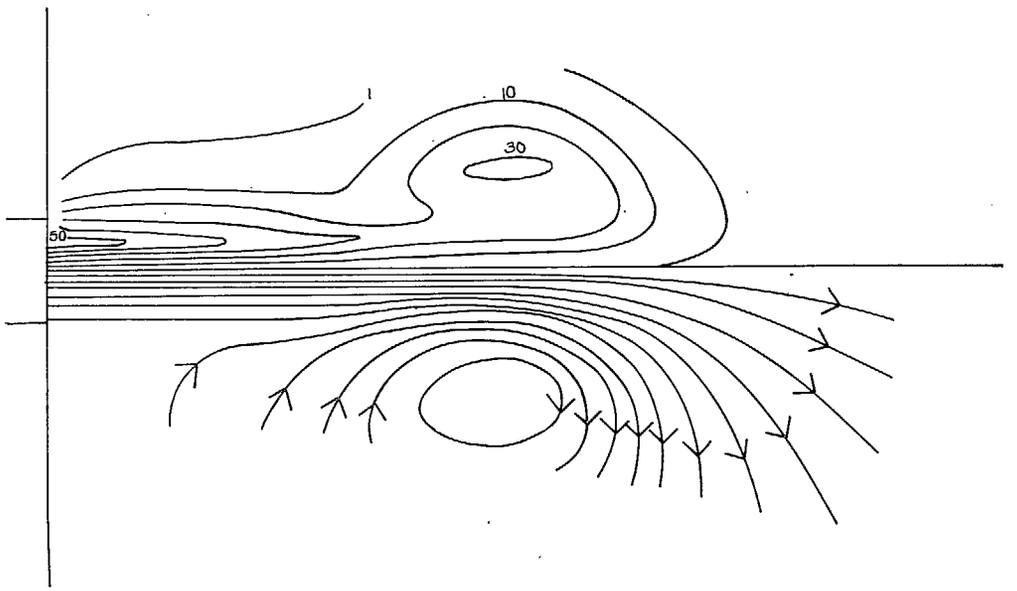

GRAPH 4.

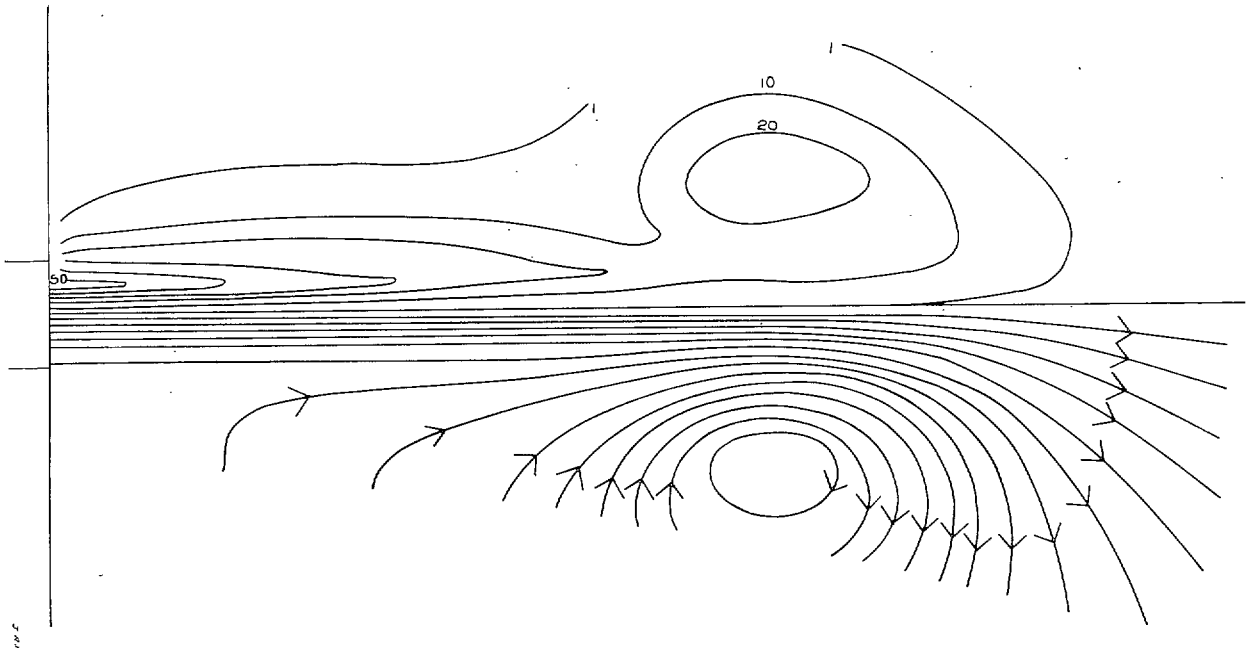

GRAPH 5.

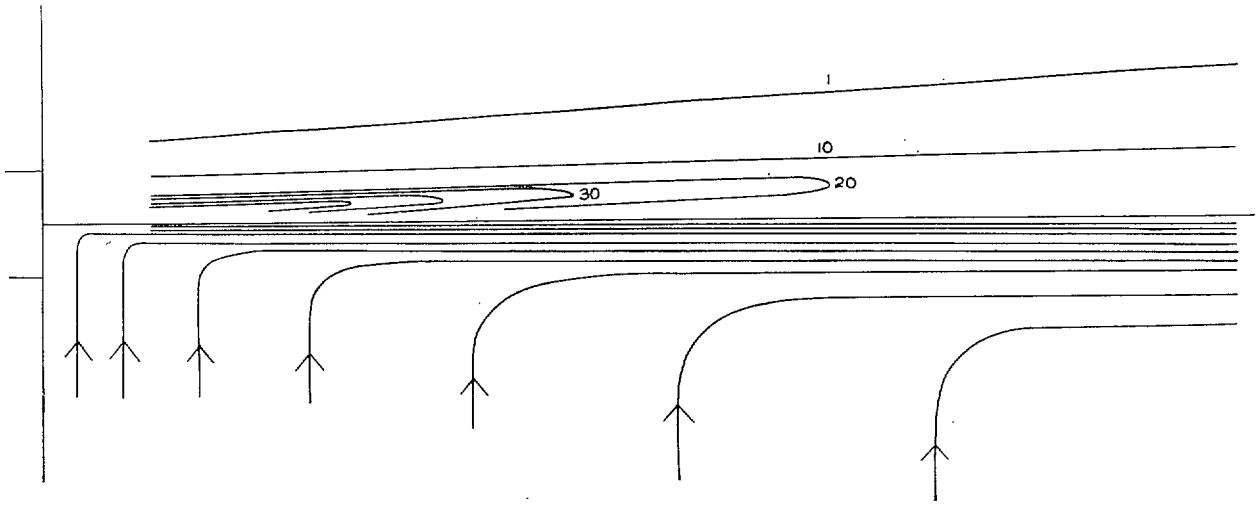

GRAPH 6.

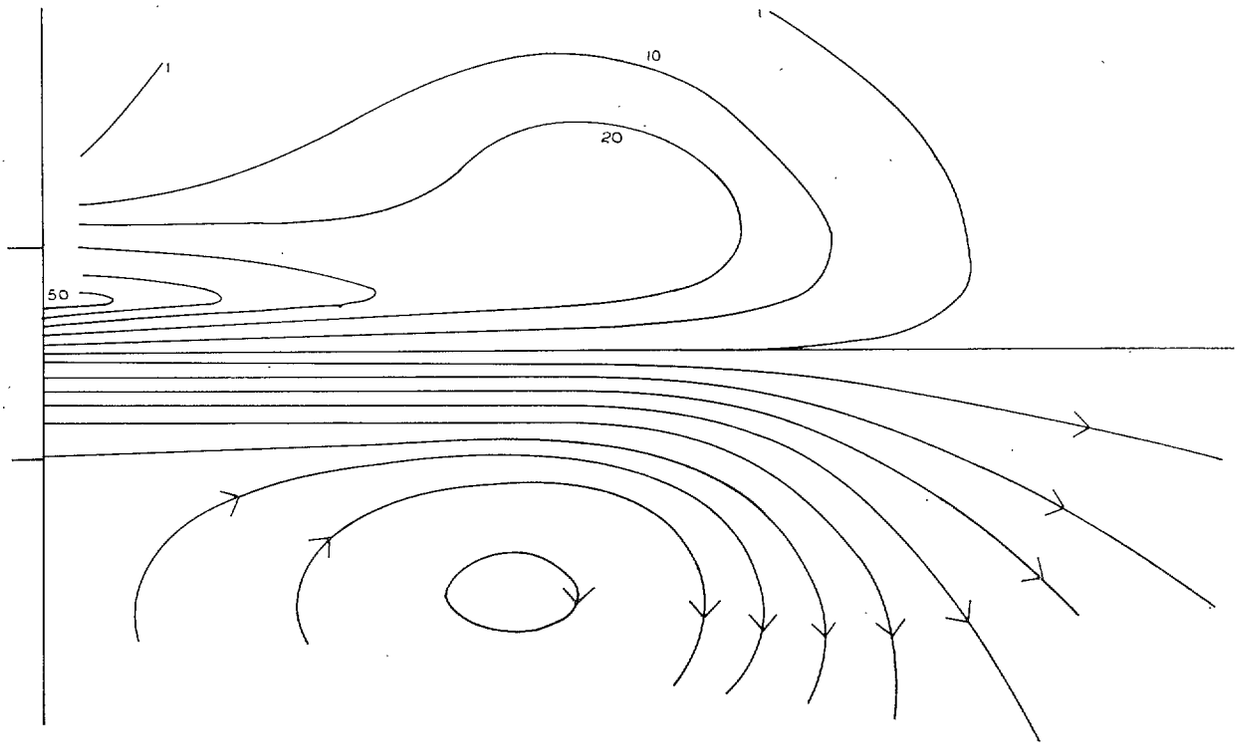

GRAPH 7.

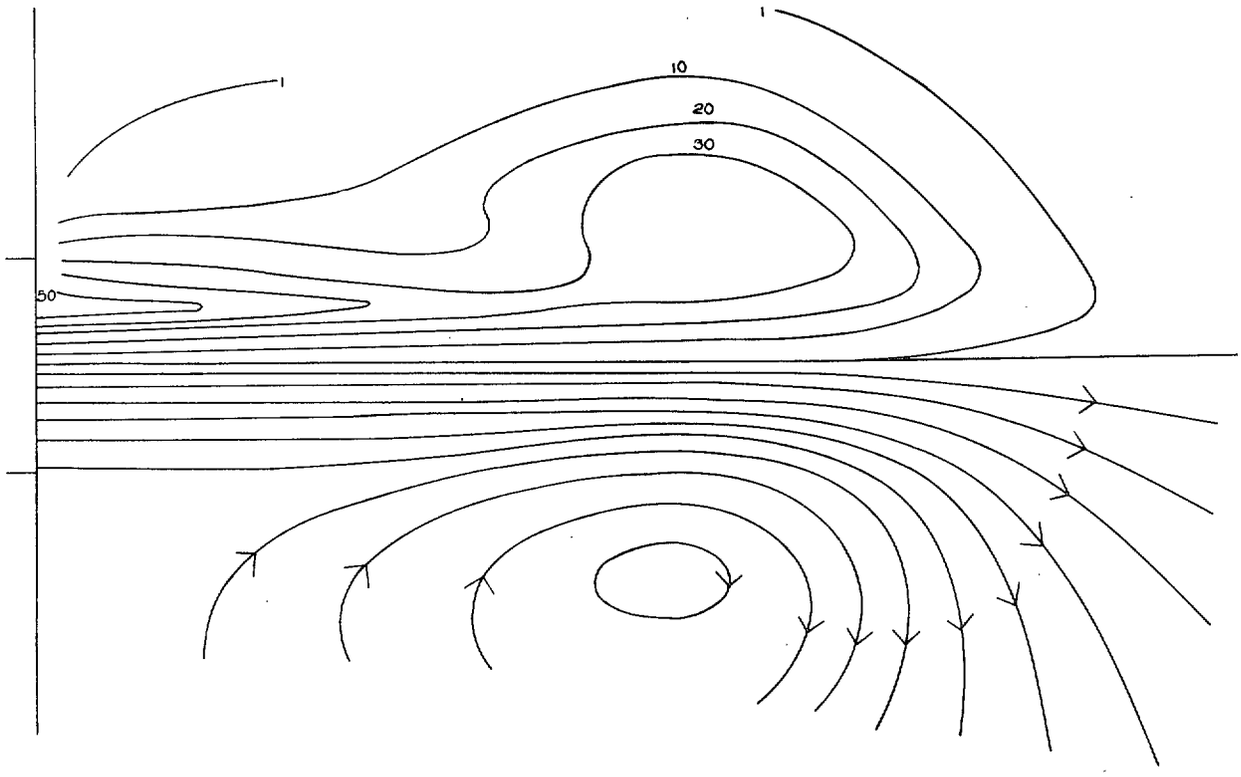

GRAPH 8.

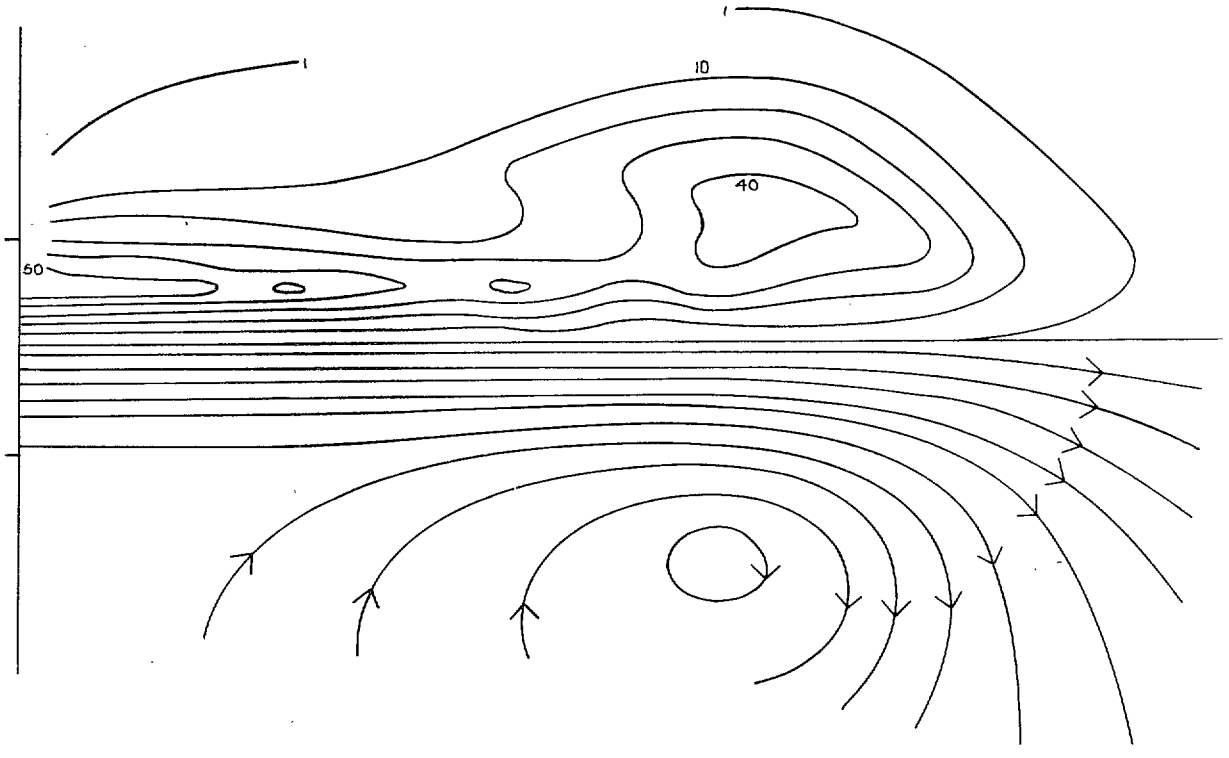

GRAPH 9.

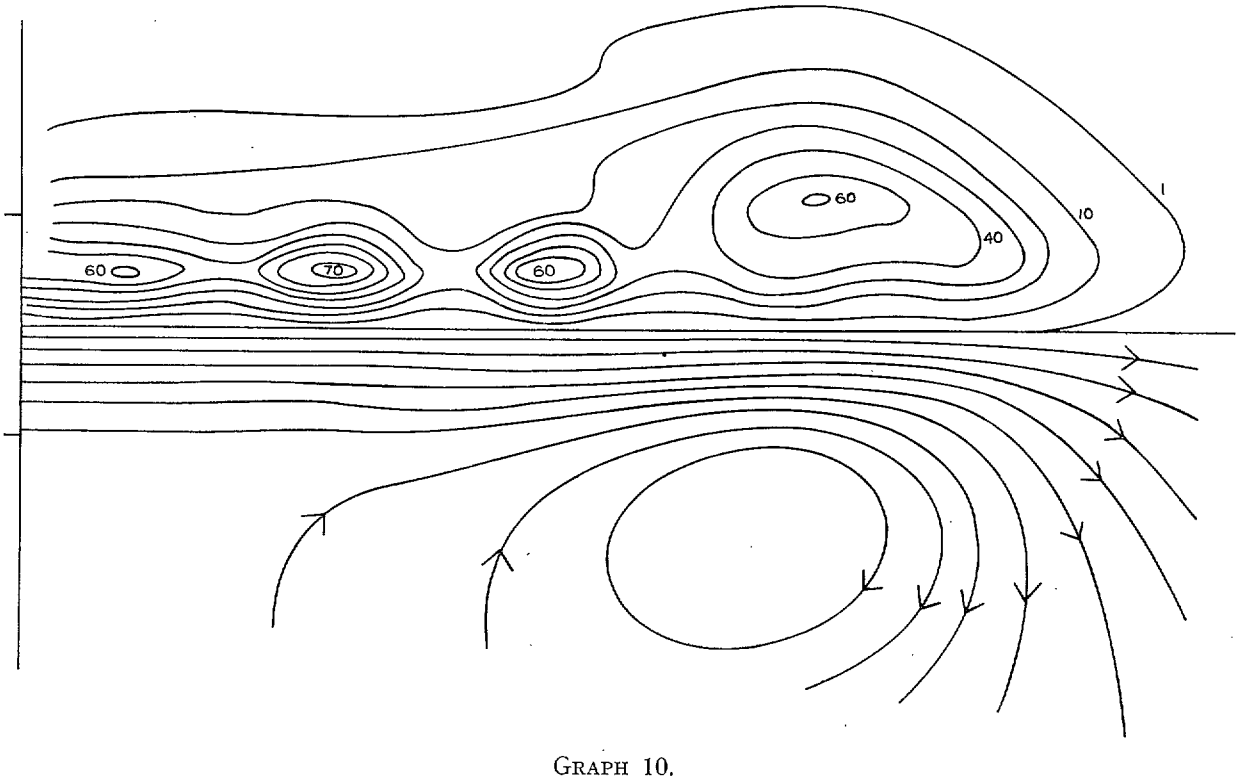

GRAPH 10.

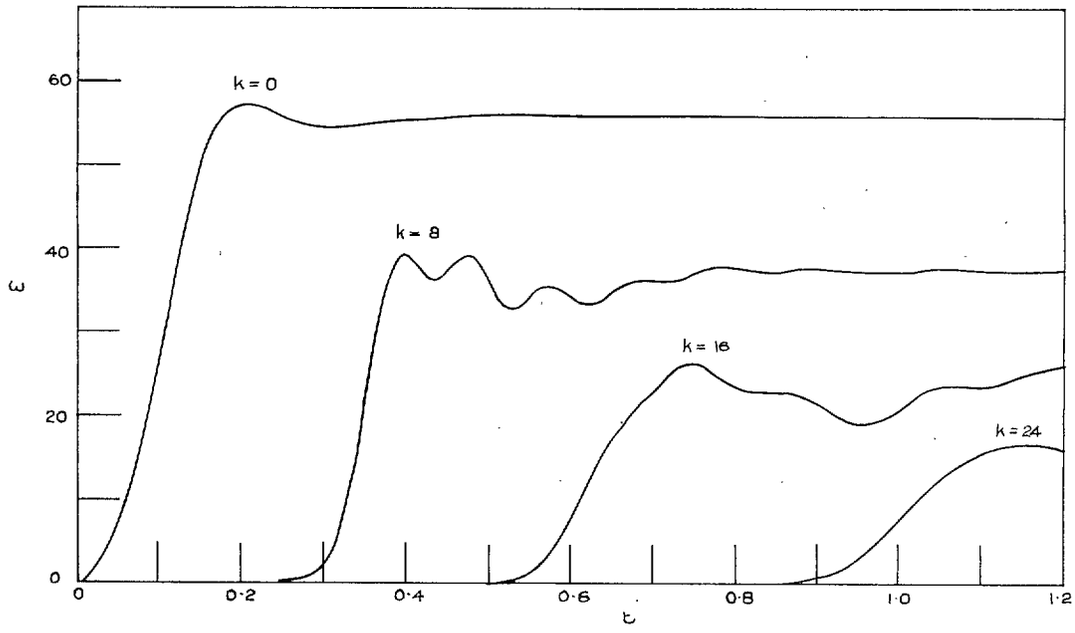

GRAPH 11.

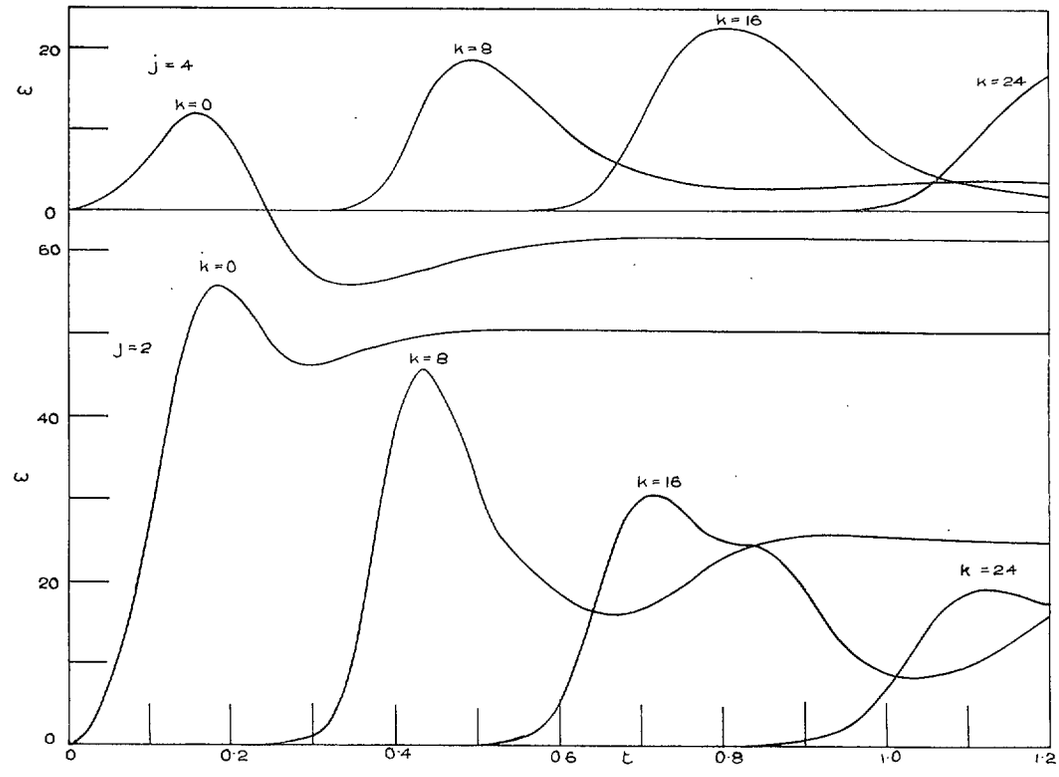

GRAPH 12.

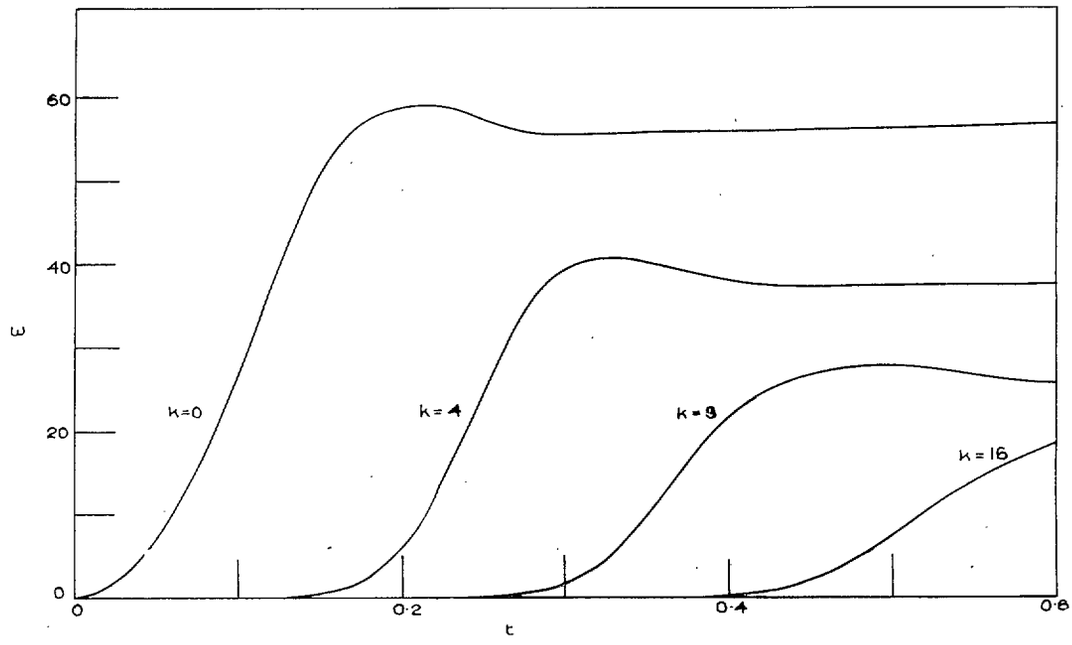

GRAPH 13.

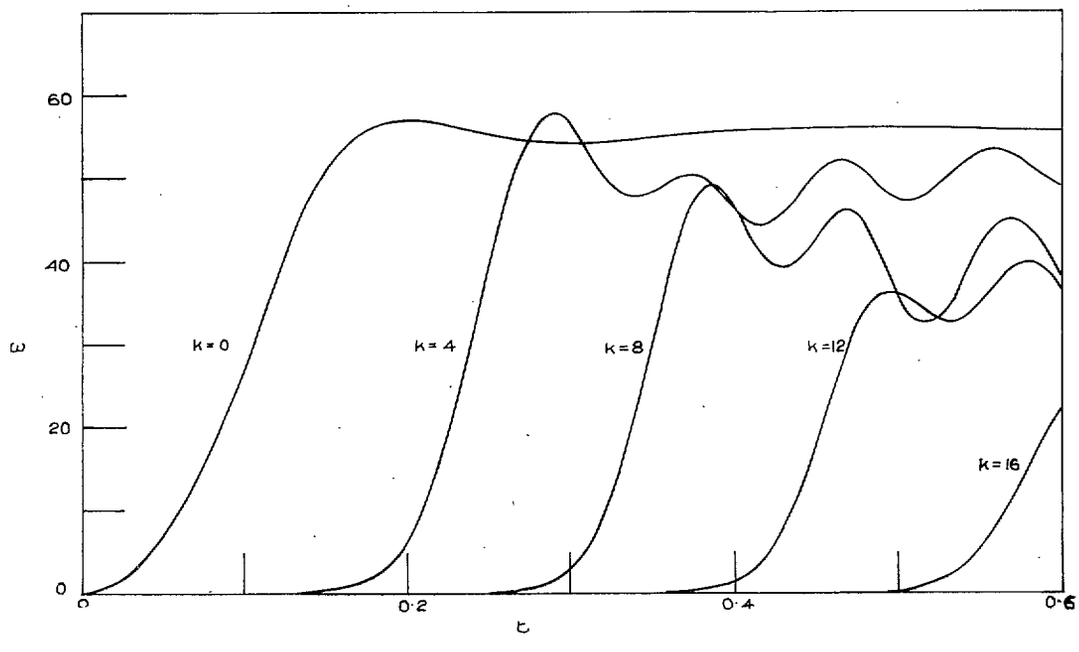

GRAPH 14.

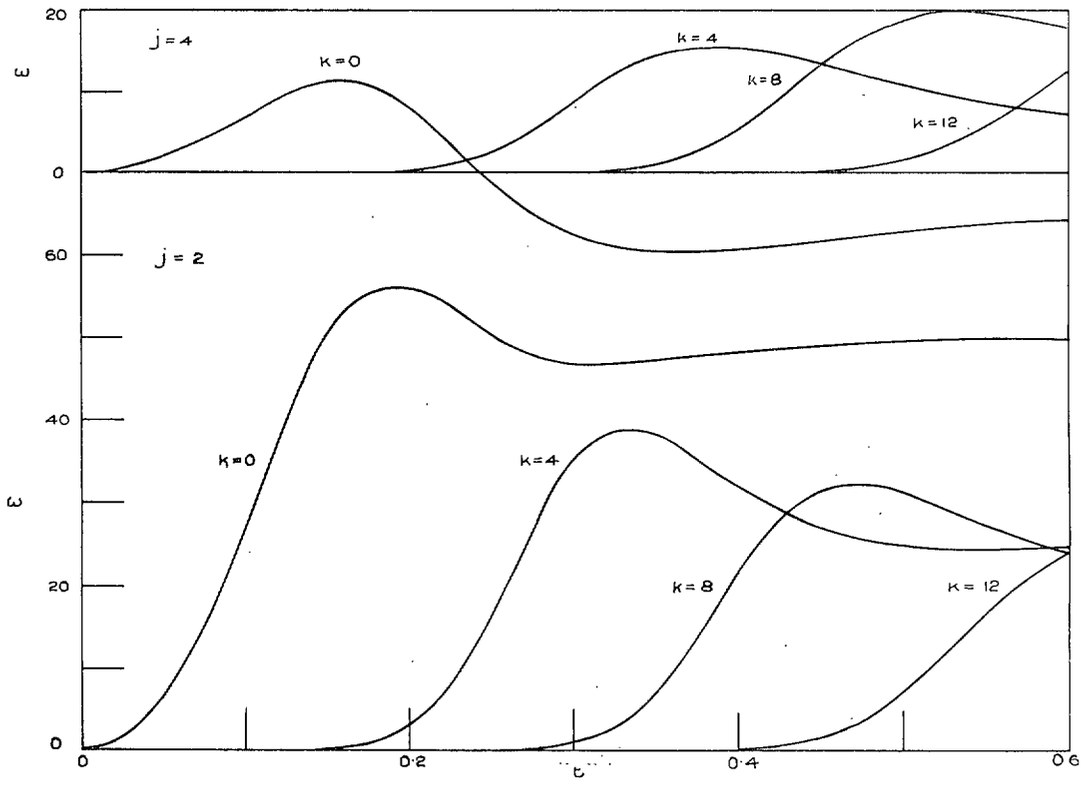

GRAPH 15.

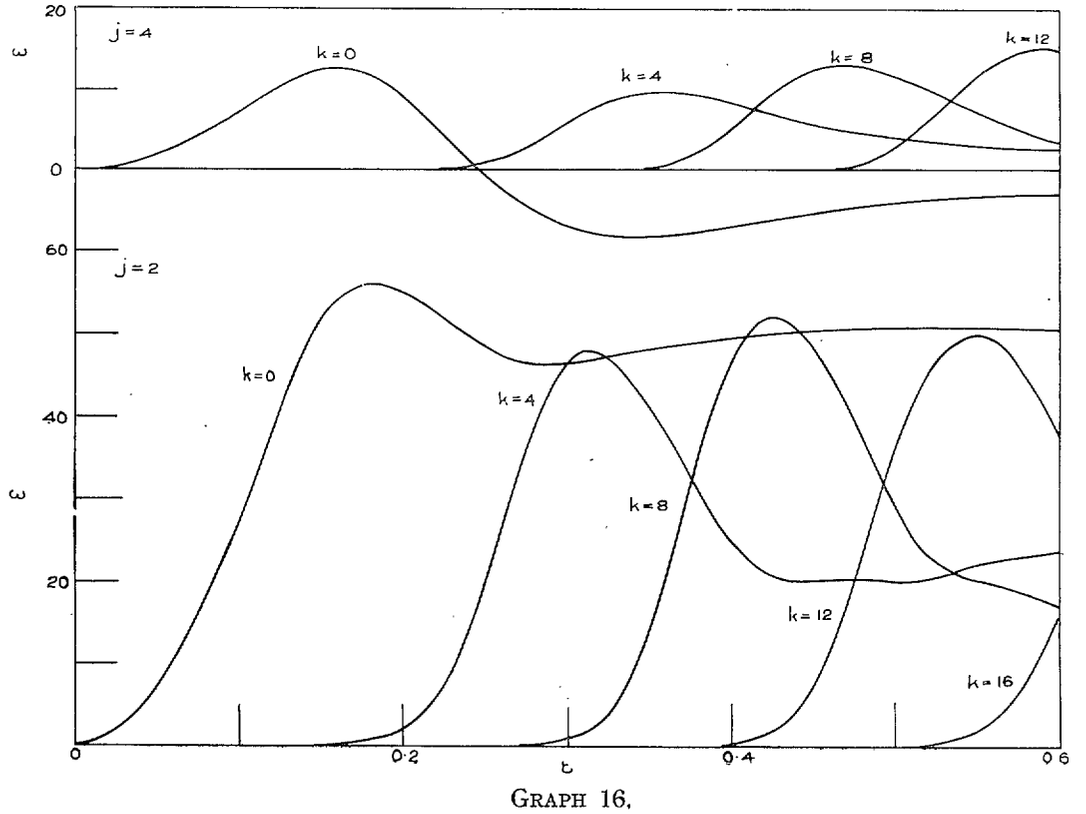

GRAPH 16.

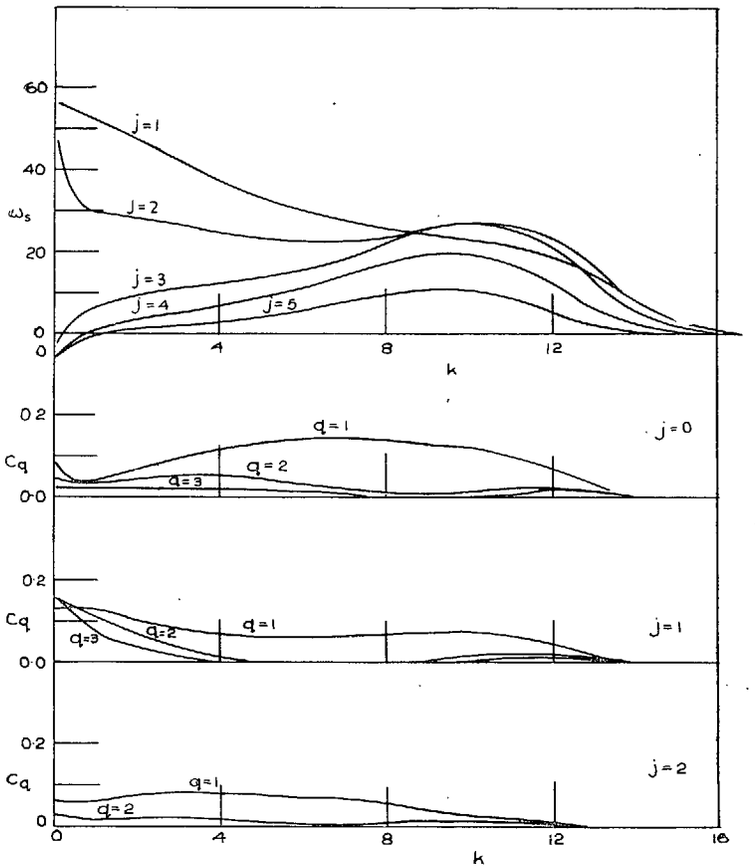

GRAPH 17.

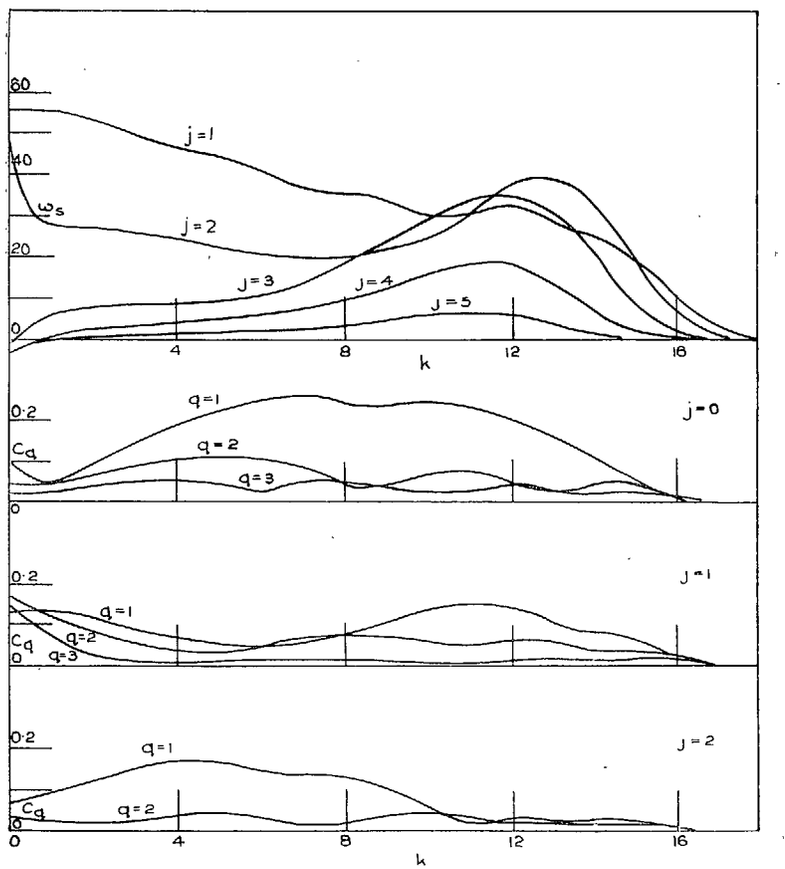

GRAPH 18.

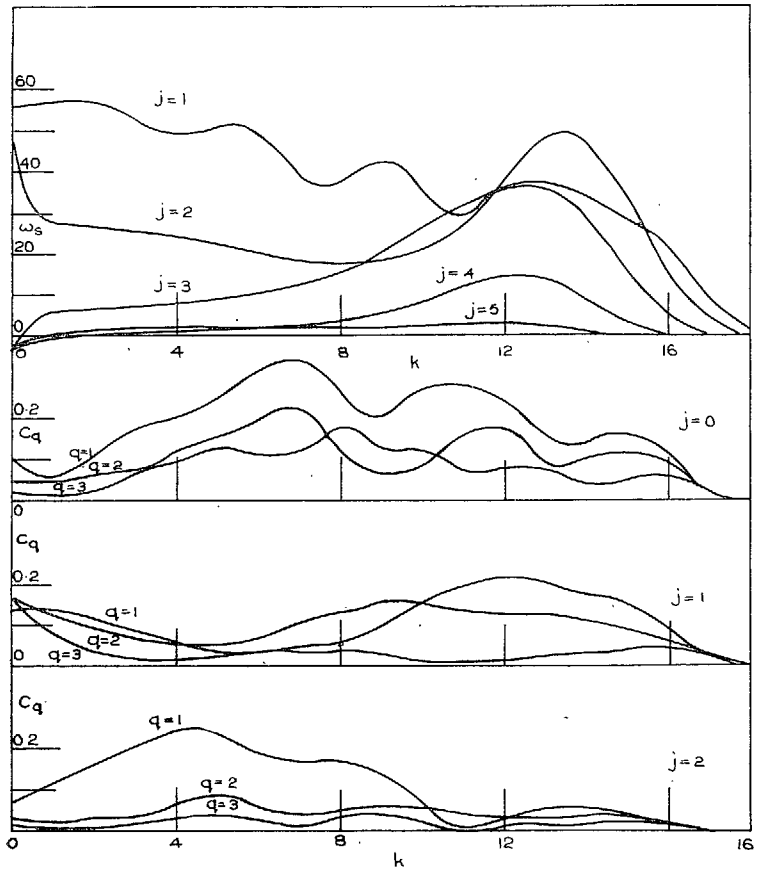

GRAPH 19.

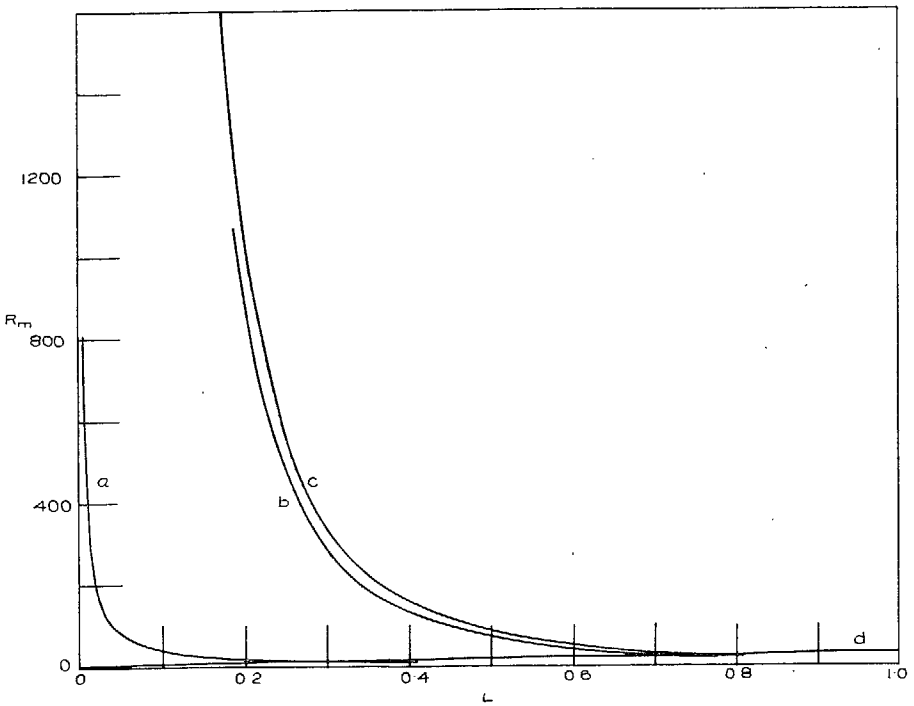

GRAPH 20.

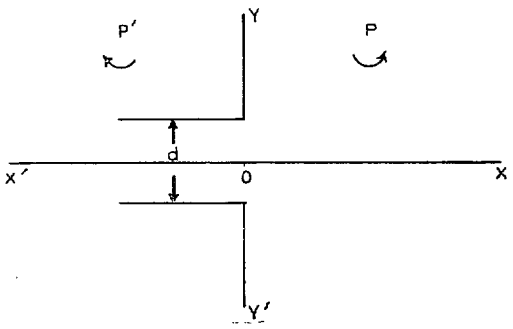

FIG. 1.

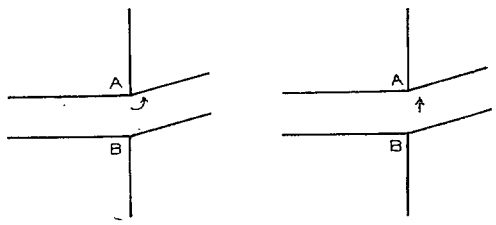

FIGS. 2 and 3.

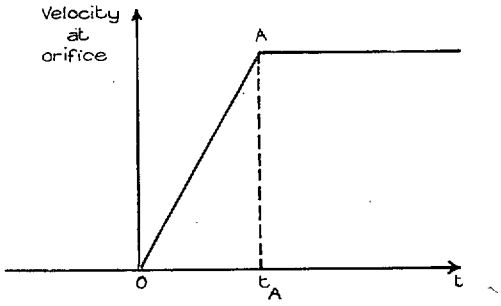

FIG. 4.

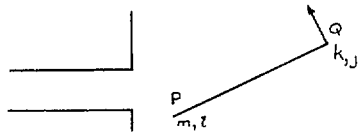

FIG. 5.

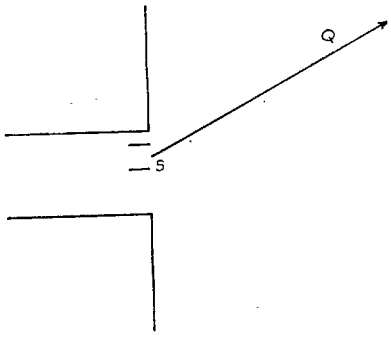

FIG. 6.

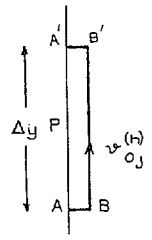

FIG. 7.

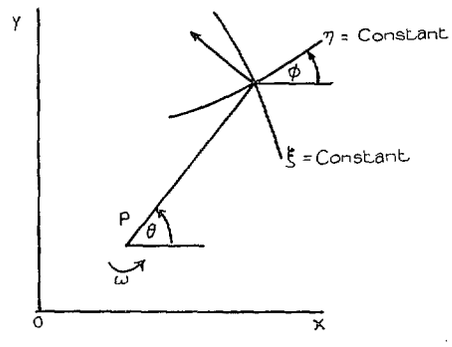

FIG. 8.

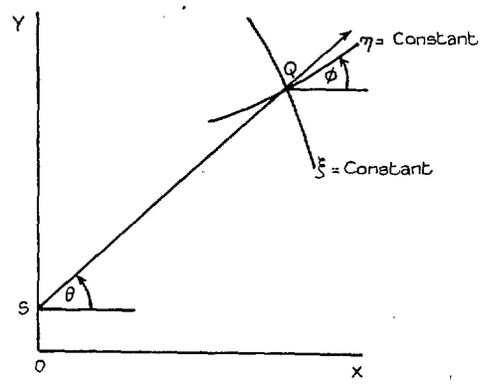

FIG. 9.

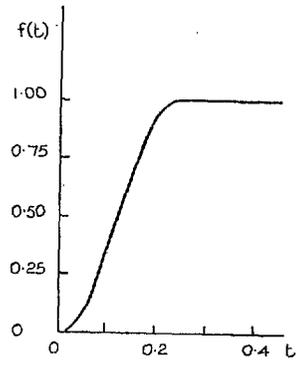

FIG. 10.

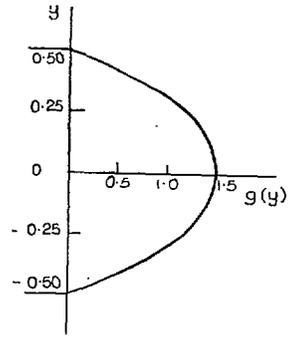

FIG. 11.

(41292) Wt. 52 K7 7/57 F. M. & S.

PRINTED IN GREAT BRITAIN

Publication of the Aeronautical Research Council

ANNUAL TECHNICAL REPORTS OF THE AERONAUTICAL RESEARCH COUNCIL (BOUND VOLUMES)

1939 Vol. I. Aerodynamics General, Performance, Airscrews, Engines. 50*s.* (51*s.* 9*d.*).
Vol. II. Stability and Control, Flutter and Vibration, Instruments, Structures, Seaplanes, etc. 63*s.* (64*s.* 9*d.*)

1940 Aero and Hydrodynamics, Aerofoils, Airscrews, Engines, Flutter, Icing, Stability and Control Structures, and a miscellaneous section. 50*s.* (51*s.* 9*d.*)

1941 Aero and Hydrodynamics, Aerofoils, Airscrews, Engines, Flutter, Stability and Control Structures. 63*s.* (64*s.* 9*d.*)

1942 Vol. I. Aero and Hydrodynamics, Aerofoils, Airscrews, Engines. 75*s.* (76*s.* 9*d.*)
Vol. II. Noise, Parachutes, Stability and Control, Structures, Vibration, Wind Tunnels. 47*s.* 6*d.* (49*s.* 3*d.*)

1943 Vol. I. Aerodynamics, Aerofoils, Airscrews. 80*s.* (81*s.* 9*d.*)
Vol. II. Engines, Flutter, Materials, Parachutes, Performance, Stability and Control, Structures. 90*s.* (92*s.* 6*d.*)

1944 Vol. I. Aero and Hydrodynamics, Aerofoils, Aircraft, Airscrews, Controls. 84*s.* (86*s.* 3*d.*)
Vol. II. Flutter and Vibration, Materials, Miscellaneous, Navigation, Parachutes, Performance, Plates and Panels, Stability, Structures, Test Equipment, Wind Tunnels. 84*s.* (86*s.* 3*d.*)

1945 Vol. I. Aero and Hydrodynamics, Aerofoils. 130*s.* (132*s.* 6*d.*)
Vol. II. Aircraft, Airscrews, Controls. 130*s.* (132*s.* 6*d.*)
Vol. III. Flutter and Vibration, Instruments, Miscellaneous, Parachutes, Plates and Panels, Propulsion. 130*s.* (132*s.* 3*d.*)
Vol. IV. Stability, Structures, Wind Tunnels, Wind Tunnel Technique. 130*s.* (132*s.* 3*d.*)

Annual Reports of the Aeronautical Research Council—
1937 2*s.* (2*s.* 2*d.*) 1938 1*s.* 6*d.* (1*s.* 8*d.*) 1939–48 3*s.* (3*s.* 3*d.*)

Index to all Reports and Memoranda published in the Annual Technical Reports, and separately—
April, 1950 - - - - R. & M. 2600 2*s.* 6*d.* (2*s.* 8*d.*)

Author Index to all Reports and Memoranda of the Aeronautical Research Council—
1909—January, 1954 R. & M. No. 2570 15*s.* (15*s.* 6*d.*)

Indexes to the Technical Reports of the Aeronautical Research Council—

December 1, 1936—June 30, 1939	R. & M. No. 1850	1*s.* 3*d.* (1*s.* 5*d.*)
July 1, 1939–June 30, 1945	R. & M. No. 1950	1*s.* (1*s.* 2*d.*)
July 1, 1945—June 30, 1946	R. & M. No. 2050	1*s.* (1*s.* 2*d.*)
July 1, 1946—December 31, 1946	R. & M. No. 2150	1*s.* 3*d.* (1*s.* 5*d.*)
January 1, 1947—June 30, 1947	R. & M. No. 2250	1*s.* 3*d.* (1*s.* 5*d.*)

Published Reports and Memoranda of the Aeronautical Research Council—

Between Nos. 2251–2349	R. & M. No. 2350	1*s.* 9*d.* (1*s.* 11*d.*)
Between Nos. 2351–2449	R. & M. No. 2450	2*s.* (2*s.* 2*d.*)
Between Nos. 2451–2549	R. & M. No. 2550	2*s.* 6*d.* (2*s.* 8*d.*)
Between Nos. 2551–2649	R. & M. No. 2650	2*s.* 6*d.* (2*s.* 8*d.*)

Prices in brackets include postage

HER MAJESTY'S STATIONERY OFFICE

York House, Kingsway, London W.C.2; 423 Oxford Street, London W.1 (Post Orders: P.O. Box 569, London S.E.1); 13a Castle Street, Edinburgh 2; 39 King Street, Manchester 2; 2 Edmund Street, Birmingham 3; 109 St. Mary Street, Cardiff; Tower Lane, Bristol, 1; 80 Chichester Street, Belfast, *or through any bookseller.*

S.O. Code No. 23-3047